Neurovascular Coupling Equations for Code version 3.3

Tim David and Allanah Kenny

August 26, 2021

Todo list

Contents

1 Introduction

Version 3.3 is written in Python (as opposed to Matlab) and now incorporates the ability to model somatosensory cortex stimulation as well as interneuron stimulation within the same code. In addition to version 3.1 we have added the simulation of the enzyme GABA-T which degrades GABA to succinic semialdehyde and glutamate [25, 24]

The single neurovascular unit (NVU) model originally developed by Farr and David [6] and later extended by Dormanns et al. [5], Dormanns et al. [4], Mathias et al. [16], Kenny et al. [10], Mathias et al. [15] and most recently by Kenny (unpublished) contains 55 ordinary differential equations (ODEs) plus a large number of algebraic variables and parameters. The equations and parameters are divided into sections corresponding to different compartments and pathways of the model. Figure 1 shows the current status of the new more simplified neuron/full model (see below for details).

2 Wilson and Cowan model

The difficulty in analysing the single neuron model used by [16] to produce a viable simulation of the Berwick mouse experimental data **refrerence Berwick results here** (HbT/O/R) has encouraged us to look at both neural mass models (which essentially produce oscillations modelling α and β waves $\Rightarrow$ EEG data) and the work of Wilson and Cowan (especially their seminal 1972 paper see Biophys Jour 12 (1-24), 1972) . We concentrate here on the Wilson Cowan model (designated CW hereafter) for the time being. The derivation of the model is reproduced here for clarity and to ensure a thorough understanding of the model and its appropriateness. We define the following

- E(t) = proportion of excitatory cells firing per unit time at time t
- I(t) = proportion of inhibitory cells firing per unit time at time t

E(t)=I(t)=0 is considered the resting state and note that both E(t) and I(t) can become negative at some time.

Suppose refractory period of excitable cells is r msecs, then the proportion of cells that are in a refractory state is given by

$$\int_{t-r}^{r} E(\tau)d\tau \tag{1}$$

thus cells which are sensitive are defined as

$$1 - \int_{t-r}^{r} E(\tau)d\tau \tag{2}$$

Similarly for I(t). We define the expected proportions of either E(t) or I(t) (subpopulations) receving at least threshold excitation per unit time as a function of the average levels of excitation within the subpopulations by $\mathfrak{S}_e(x)$ and $\mathfrak{S}_i(x)$. Suppose a distribution function $\mathfrak{D}$ of individual thresholds for the subpopulation then

$$\mathfrak{S}(x) = \int_{0}^{x(t)} \mathfrak{D}(\theta)d\theta \tag{3}$$

where x(t) is the average excitation OR

$$\mathfrak{S}(x) = \int_{\frac{\theta}{x(t)}}^{\infty} \mathfrak{C}(\omega)d\omega \tag{4}$$

where $\mathfrak{C}(\omega)$ is a distributions of synapses per cell. Both definitions produce (if $\mathfrak{D}, \mathfrak{C}$ are monotonic) an $\mathfrak{S}(x)$ which is sigmoidal in shape. We can write this as

$$\mathfrak{S}(x) = \frac{1}{1 + exp[-\gamma(x - \delta)]} \tag{5}$$

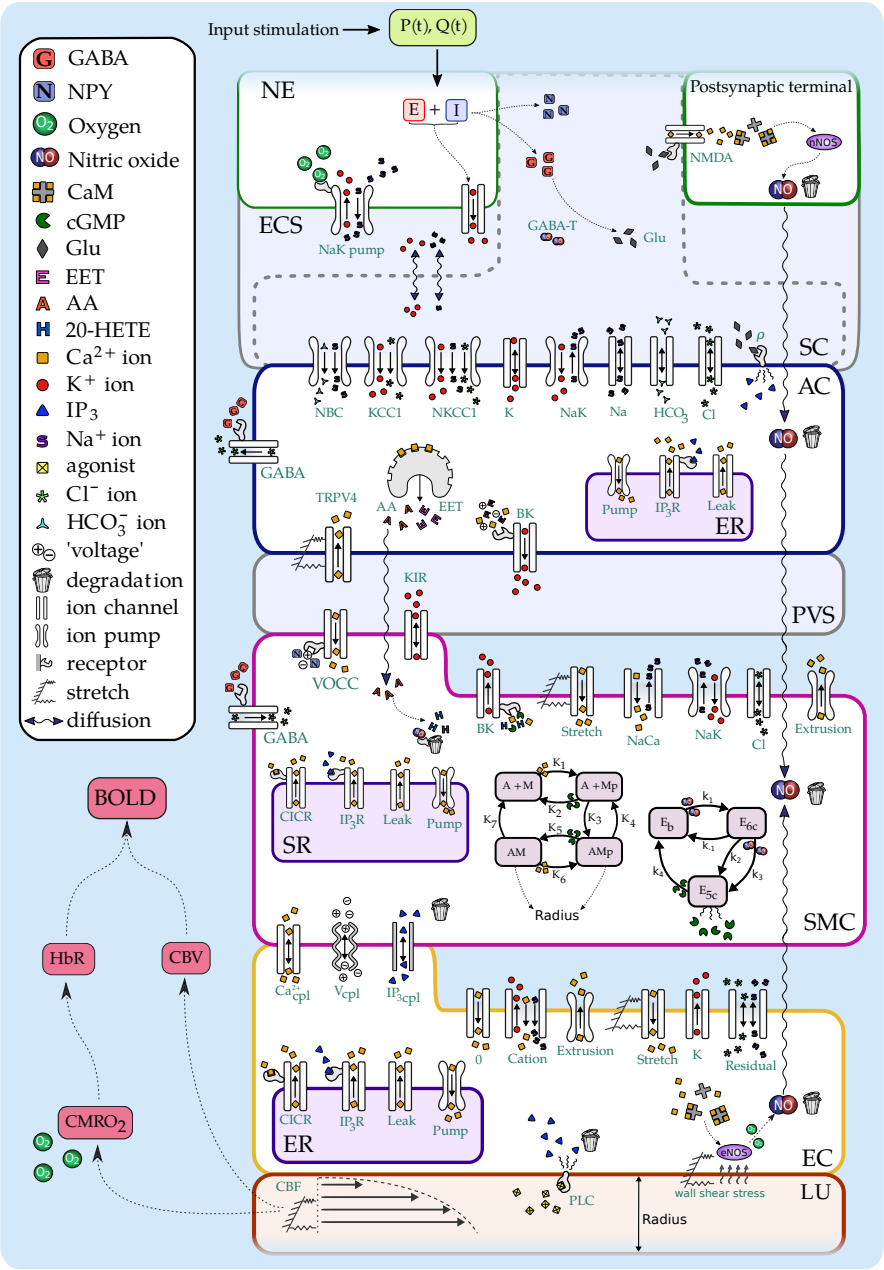

Figure 1: **FULL** NVU 3.3 including BOLD pathway and Wilson and Cowan neuron model

Assuming individual cells sum their inputs and the delay from stimulation is $\alpha(t)$ then the average level of excitation generated will be

$$\int_{-\infty}^{t} \alpha(t-\tau)[c_1 E(\tau) - c_2 I(\tau) + P(\tau)]d\tau \tag{6}$$

c_1 and c_2 represent the average number of excitatory/inhibitory synapses per cell and $P(\tau)$ is the external input to the excitatory subpopulation. By assuming a "coarse grain" variable defined by

$$\bar{f}(t) = \frac{1}{s}\int_{t-s}^{t} f(\tau)d\tau \tag{7}$$

and assuming that at time t+τ the dynamics of the localised populations are given by

$$E(t+\tau) = \left[1 - \int_{t-r}^{t} E(t')dt'\right] \mathfrak{S}_e(x_e(t)) \tag{8}$$

with x(t) defined previously, and

$$I(t+\tau) = \left[1 - \int_{t-r}^{t} I(t')dt'\right] \mathfrak{S}_i(x_e(t)) \tag{9}$$

Using Taylor series expansion about τ=0 gives

$$\begin{aligned} \tau \frac{dE}{dt} &= -\bar{E} + (1 - r\bar{E})\mathfrak{S}_e\left[kc_1\bar{E} - c_2\bar{I} + kP(t)\right] \\ \tau' \frac{dI}{dt} &= -\bar{I} + (1 - r\bar{I})\mathfrak{S}_i\left[k'c_3\bar{E} - c_4\bar{I} + k'Q(t)\right] \end{aligned} \tag{10}$$

Q(t) is the stimulation of the inhibitory cells and

$$\begin{aligned} \int_{t-r}^{t} E(t')dt' &= r\bar{E} \\ \int_{-\infty}^{t} \alpha(t-t')E(t')dt' &= k\bar{E} \end{aligned} \tag{11}$$

With some redefinitions we have the final odes

$$\begin{aligned} \tau_e \frac{dE}{dt} &= -E + (k_e - r_e E)\mathfrak{S}_e\left[c_1 E - c_2 I + P(t)\right] \\ \tau_i \frac{dI}{dt} &= -\bar{I} + (k_i - r_i I)\mathfrak{S}_i\left[c_3 E - c_4 I + Q(t)\right] \end{aligned} \tag{12}$$

We should note the following . The state E=I=0 should be stable and be a steady state solution to equations 2 for P=Q=0. $\mathfrak{S}_e$ and $\mathfrak{S}_i$ are transformed so that $\mathfrak{S}_e = \mathfrak{S}_i = 0$. This gives

$$\mathfrak{S}(x) = \frac{1}{1 + exp[-\alpha(x-\delta)]} - \frac{1}{1 + exp(\alpha\delta)} \tag{13}$$

But the maximum values of $\mathfrak{S}_{e,i}$ will be less than zero and hence k_e and k_i are the max values. as defined

$$\lim_{x\to\infty} \mathfrak{S}(x) = 1 - \frac{1}{1 + exp(\alpha\delta)} \tag{14}$$

The isoclines for the equations 2 suggest that $\exists$ 3 or possibly 5 steady states. In our case we wish to progress from E=I=0 when P=Q=0 to some stable state with P,Q, $\neq$0 and for the system to return to E=I=0. This is not trivial (see Wilson and Cowan paper). However using the following parameters we have been able to produce a reasonable profile for E(t) and I(t)

Table 1

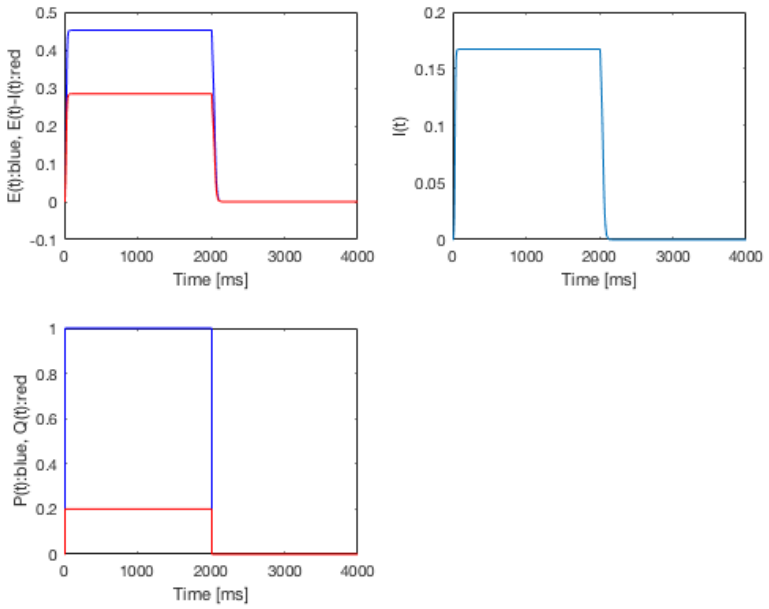

Figure 2: Upper left: E(t) and E(t)-I(t), Upper right: I(t). Lower left P(t) and Q(t)

Parameter	Value
c_1	12
c_2	10
c_3	13
c_4	11
a_e	1.2
θ_e	2.8
a_i	1.0
θ_i	4.0
r_e	1.0
r_i	4.0
τ_e	10 msecs
τ_i	10 msecs

$k_e = \mathfrak{S}_e(10)$ and $k_i = \mathfrak{S}_i(10)$ are used to produce maximum values of the sigmoid function. Both k_e and k_i are ¡ 1. We should note here that due to the small values of the characteristic time scales τ_e and τ_1 the output for E and I are essnetially 'square pulses' if the functions P and Q are also 'square pulses' and the stimulation period is much larger than τ_e or τ_i. Figure 2 shows the results of E(t) and I(t) for a 2 second stimulation

Note that the horizontal axes are in milliseconds. In order to develop the neuron model further we need to ensure that the more simple model replicates (adequately) the results of the more complex one. It turns out (see below the section in determining the ATP-ase pump) that in order to develop this simple model all that is needed are four outputs, viz. K^+ in the ECS, Na^+ in the soma and dendrite and the time derivative of the K^+ in the ECS.
We show the output of the full single neuron model for 2 (Figure 3) and 16 second (Figure 4) stimuli. K^+ in the synaptic cleft is determined from the derivative of the potassium (K^+) in the ECS. It is important to make sure that the resulting K^+ replicates adequately the result of Ostby [18], since we know this works !!
It can be seen that the profiles for K^+ and both sodium (Na^+) could be modelled using a differential equation of the

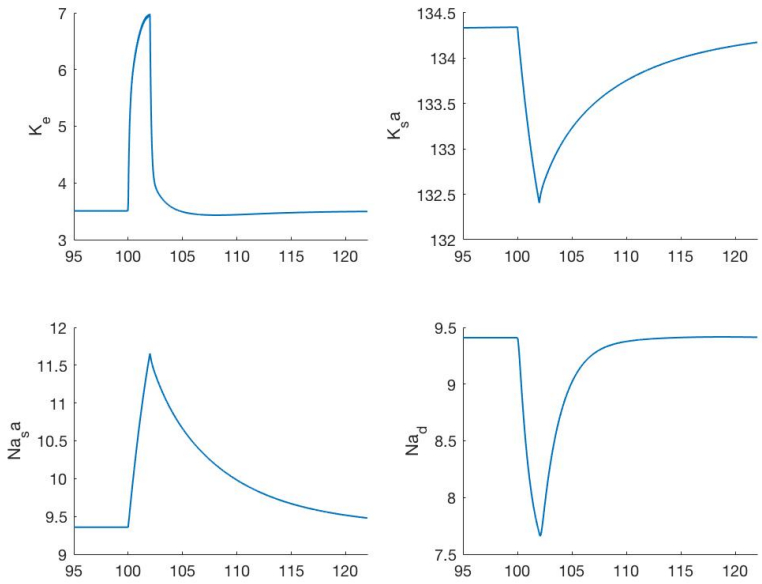

Figure 3: Time-dependent profiles of a 2 sec stimulus for K^+ in the ECS and the synapse of the neuron (top row) and Na^+ in the soma and dendrite (bottom row). **Simulation from the single neuron model**

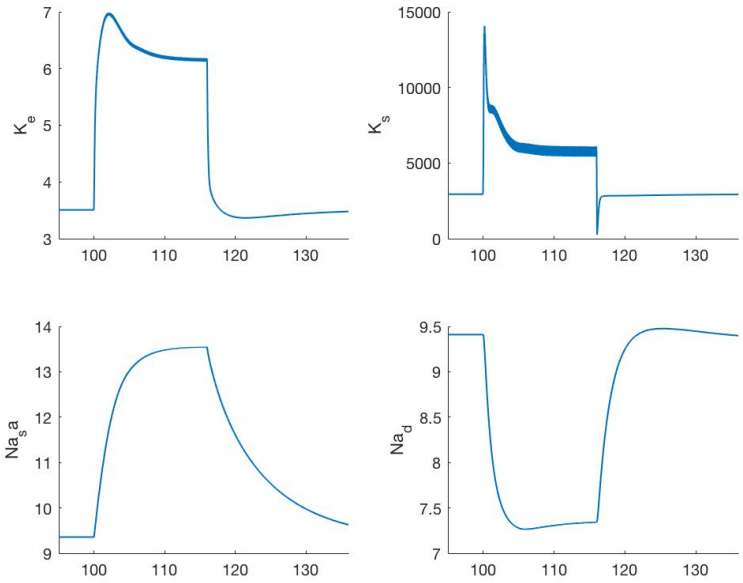

Figure 4: Time-dependent profiles of a 16 sec stimulus for K^+ in the ECS and the synapse of the neuron (top row) and Na^+ in the soma and dendrite (bottom row).**Simulation from the single neuron model of Mathias [16]**

form

$$\frac{d\phi_i(t)}{dt} + \alpha_i \phi(t) = f_i(t) \tag{15}$$

Furthermore $f_i(t)$ could be found using the profiles of E(t) and I(t). Such that

$$f_i(t) = f_i(E(t) - I(t)) \tag{16}$$

The general solution looks like

$$\phi_i(t) = \frac{f_i(t)}{\alpha_i}\left(1 - exp(-\alpha_i t)\right) \tag{17}$$

or more succintly

$$\frac{d\phi_i(t)}{dt} + \beta\phi = \alpha\beta \tag{18}$$

with solution

$$\phi_i(t) = \alpha\left(1 - exp(-\beta t)\right) \tag{19}$$

We are now in a position to develop a simple neuron model. Some experiments have provided information with which we can establish adequate values for α and β. We assume that the forcing function (RHS of ode) is a 'square wave'. We further assume that the stimulus is of the order of 0.022 mA cm^{-2}. On this basis the functions modelling K^+ and Na^+ are given by

$$\begin{aligned}\left[K_e^+\right](t) &\simeq 3.5 + 2.7(1 - exp(-1.5t))\\ \left[Na_d^+\right](t) &\simeq 9.42 - 2.12(1 - exp(-0.7t))\\ \left[K_{sa}^+\right](t) &\simeq 9.37 + 4.23(1 - exp(-0.65t))\end{aligned} \tag{20}$$

We now use the values of the parameters listed in Table 1 above and those in equation 20 since these replicate the original single neuron model output and find the solution to the time-dependent profiles for K_e^+,Na_{sa}^+ and Na_d^+ using various values of P(t) to signify a varying stimulus magnitude and the forcing function given by $\delta(E(t) - I(t))$ where for a stimulus of 0.022 mA cm^{-2} the forcing function is of unit magnitude. This value of 0.022 mA cm^{-2} was the original value when using the Mathias neuron model. There is a clear bifurcation at P(t)$\simeq$0.4 . This is expected as Wilson and Cowan show that the steady state values traverse from stable through unstable to stable again as P(t) moves from 0.3 to higher values. As shown in Figure 5. We assume WLOG that P(t)=0.5 correpsonds to a stimulus of 22 mA cm^2. Varying the value of P(t) therefore enables the model to vary the stimulus input magnitude.

In the Ostby model the input to the NVU system was essentially a flux of K^+ into the synaptic cleft. In the Mathias neuron model this was achieved by using the derivative of the ECS K^+ multiplied by a constant to take into account the small syaptic volume compared to that of the ECS. We therefore need to determine the time dependent value of $\frac{dK_e^+}{dt}$. This is trivial as it is just a rearrangement of the ode given in equation 2. It is written as

$$\frac{dK_e^+}{dt} = -\beta K_e^+ + \alpha\beta \tag{21}$$

Figure 6 shows the derivative $\frac{dK_e^+}{dt}$ as a function of time. This should be compared to the Ostby input as shown in Figure 7. Note that the time scales are different but the essential form is similar. And the integrals of the positive value of $\frac{dK_e^+}{dt}$ is equal to the negative vaue of $\frac{dK_e^+}{dt}$ as is the case with Ostby.

3 Results from Wilson and Cowan model

We are now in a position to compare the new neuron model developed from Wilson and Cowan with experimental results from [32]. Firstly Figure 8 shows the excitatory and inhibitory inputs E(t) and I(t) resp. All figures show the old model in red and new model in blue. Figure 9 shows the flux of K^+ into the synaptic cleft for the old neuron model [16] (red) compared with the new model (blue). Figure 10 shows the K^+ in the ECS for both models (colours as noted above). Figure 3 shows the K^+ in the synaptic cleft. Figure 12 shows the resulting radius (red: old model, blue: new model) Here we see that the radius now has the correct 'plateau' profile. The rate of increase at the start of the atimulation is

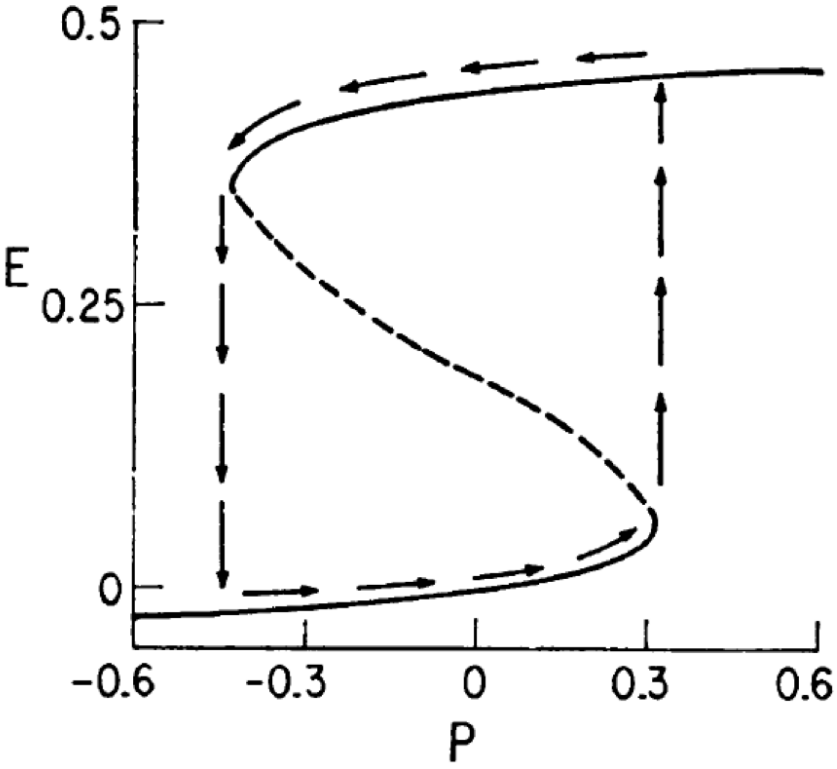

Figure 5: E vs P (taken from Wilson and Cowan paper)

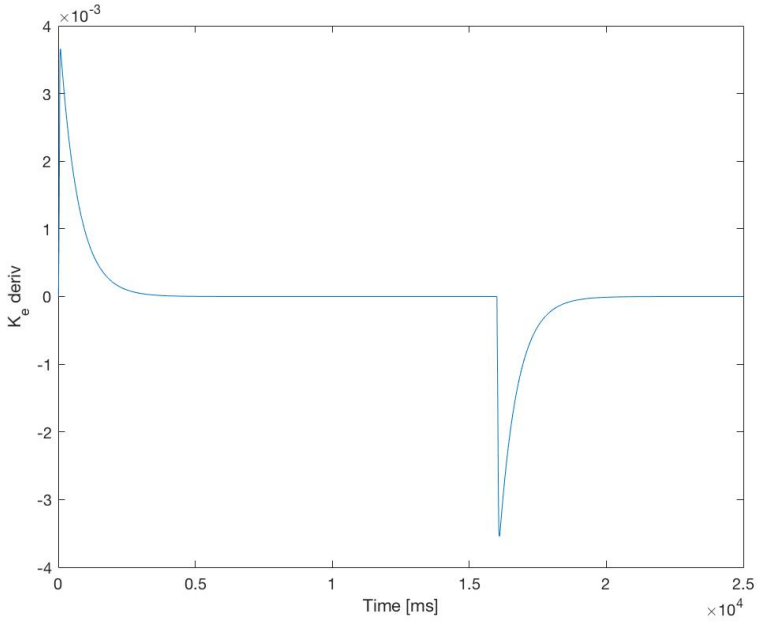

Figure 6: $\frac{dK_e^+}{dt}$ as a function of time using a stimulation of 16 seconds. re-arrangement of basic K^+ ode, see equation 2.

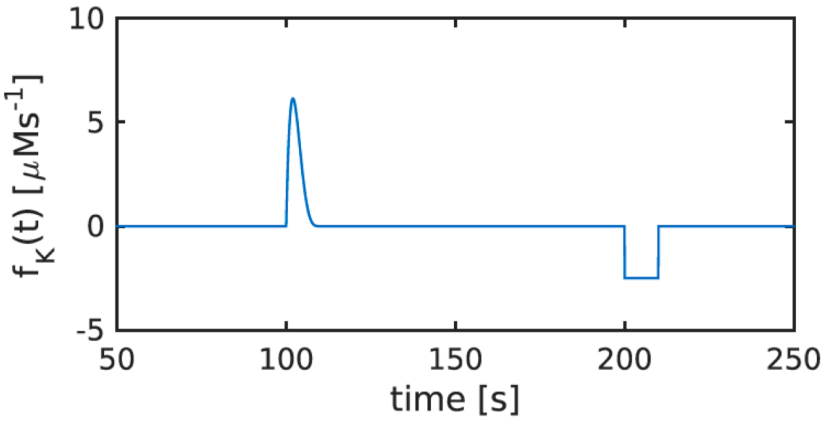

Figure 7: Ostby input (replicating a neuron activation) over 200 seconds, compare with Figure 6

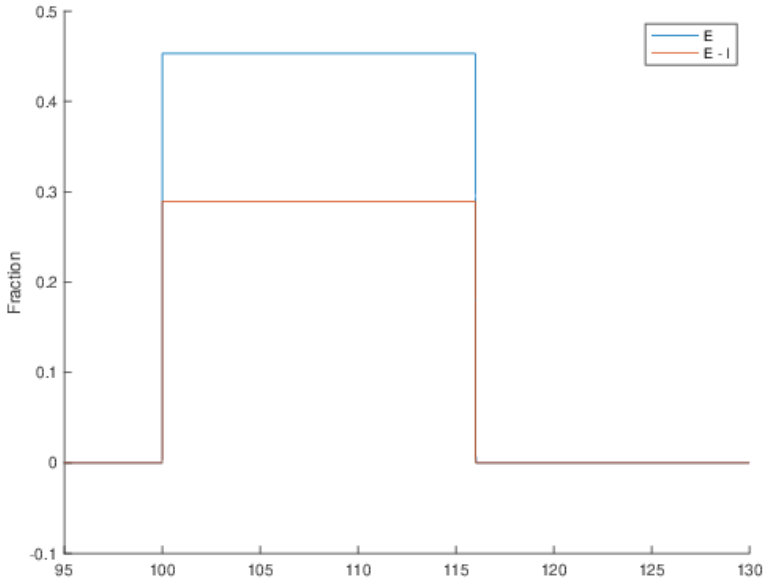

Figure 8: E(t) and I(t) for a 16 second stimulation

the same as the old model. A comparison can be done with the results of [32]. Figure 13 provides the time-dependent profiles of ΔCBF for both Zheng and the Wilson/Cowan model. The value of the K^+ in the ECS has been adjusted to make the maximum height of the ΔCBF profile fit to the experiment. We note a number of issues

- The initial rate of increase of ΔCBF is lower than the Zheng result from the experiment
- The decay of the ΔCBF is also too long.
- the model profile does not exhibit a 'dip' in the middle of the stimulus.

The ΔCBF rates in increase and decay are functions of the radius profile. We are able to change the initial rate and final decay by altering the smooth muscle mechanics. **This will be done at a later stage.** The 'dip' however can be simulated by investigating the profile of the neuronal input. We show below how this may be achieved.

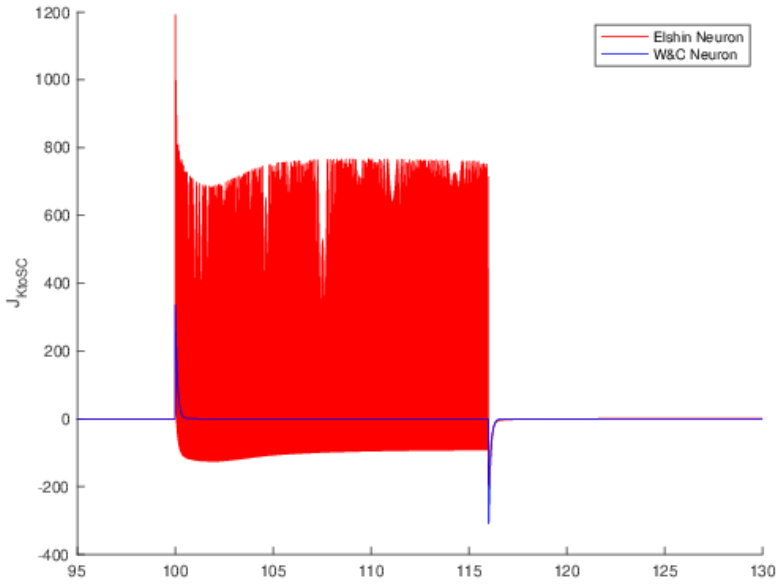

Figure 9: Flux of K+into the synaptic cleft (old model red, new model blue)

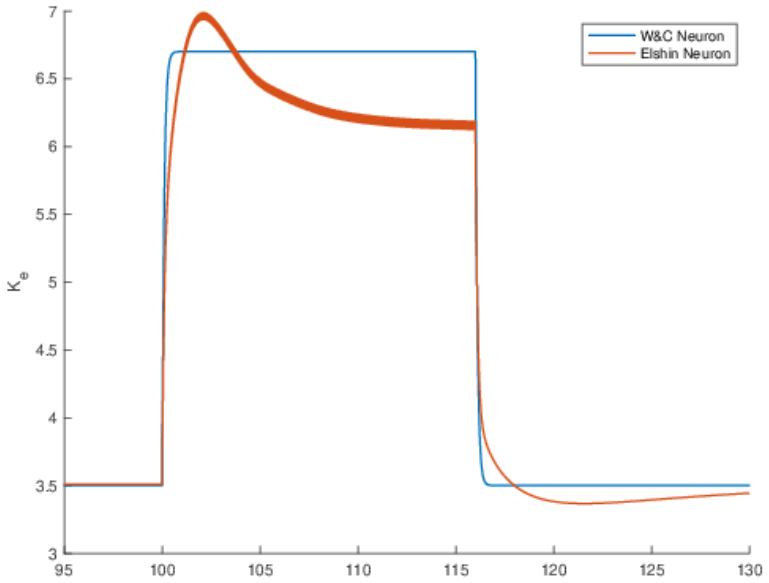

Figure 10: K+ in the ECS (red: old model. Blue: new model)

3.1 Models of Murine whisker stimulation

Chapter 11 of the book Mathematical Foundations of Neuroscience by Ermentrout and Terman provides a model of the excitatory and inhibitory neurons resulting from thalamic input as a way of describing the stimulation of the somoato-sensory cortex via the whisker pad. Within the barrel cortex of the rat there exist strong recurrent excitatory and inhibitory networks. These connected networks receive stimulus from the thalamus (T(t)). Each neuronal type inhibits

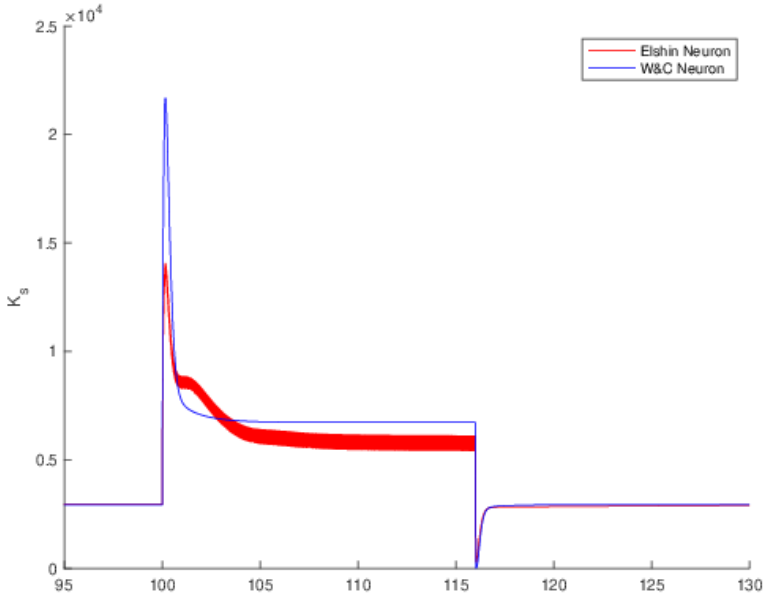

Figure 11: K+(t) in the synaptic cleft (red: old model, blue: new model)

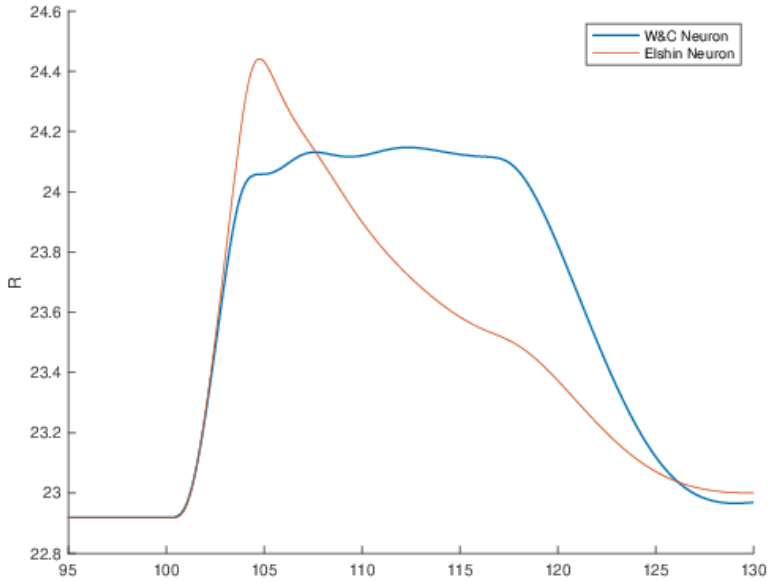

Figure 12: Radius R(t) for a 16 second stimulus (red: old model, blue: new model)

the other and themselves.

The experiments seem to show that it is not the peak value of the thalamic input but the time rate of change of the

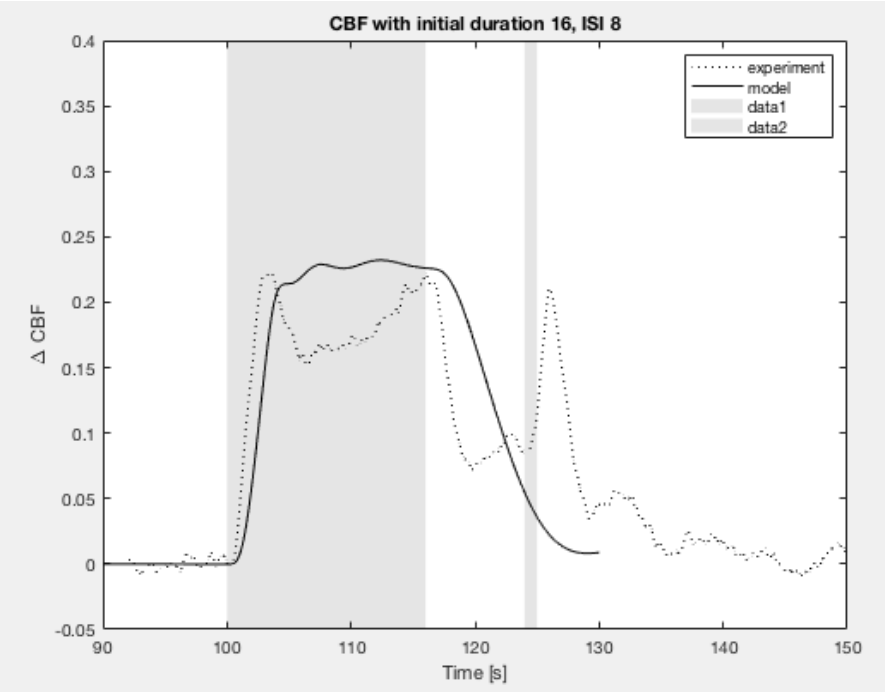

Figure 13: Comparison of old neuron model with new model for ΔCBF

stimulation. The chapter provides an example whose equations are given below.

$$\tau_e \frac{dE}{dt} = -E + F_e \left(w_{ee} E - w_{ie} + w_{te} T(t) \right) \tag{22}$$

$$\tau_i \frac{dI}{dt} = -I + F_i \left(w_{ei} E - w_{ii} + w_{ti} T(t) \right) \tag{23}$$

Table 1 (parameters for barrel cortex model)

w_{ee}	42
w_{ie}	24
$_{ei}$	42
w_{ii}	18
τ_e	5
τ_i	15
w_{te}	53.43
w_{ti}	68.4

Along with the gain functions written as

$$F_e(x) = \frac{5.12}{\left(1 + exp\left(-\frac{(x-15)}{4.16}\right)\right)} \tag{24}$$

$$F_i(x) = \frac{11.61}{\left(1 + exp\left(-\frac{(x-15)}{3.94}\right)\right)} \tag{25}$$

We should note finally that Ermentrout and Terman show that the factor $(1 - r_e E)$ makes little difference to the output so it is assumed that both r_e and $r_i = 0$.

To round out the model a thalamic input is needed. Since the rate of increase of input is the signifying factor in whether the firing rate increases a function is needed which simulates a relatively constant max value but a variation in the time

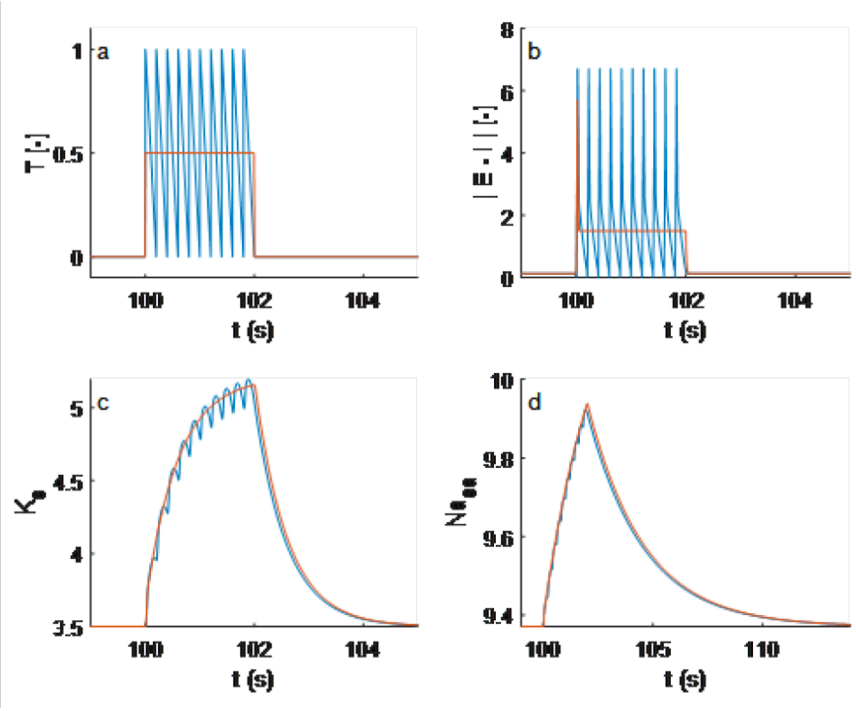

Figure 14: Comparison of WC model resulst for oscillatory thalamic input compared to an averaged value.

taken to reach that value.

Using the thalamic model parameter values and an input (triangular oscllations) similar to that derived from an experiment by Berwick et al Figure 14 shows a comparison between $\mid E(t) - I(t) \mid$, K_e, Na_{sa} as a function of T (thalamic input) as can be seen the averaged value follows closely that of the oscillatory response. We therefore conclude that using averaged values is best and saves on compute time.

4 Interneuron Modeling (essentially version 3.4)

As part of a collaboration with the Berwick group in Sheffield UK it was decided to create a model of an inhibitory interneuron with γ-aminobutyric acid (GABA) and neuropeptide Y (NPY) to induce dilation when the neuronal vascular response is mediated by GABA but provides constriction with NPY. This is clearly a balance of two competeing pathways. To produce a viable model it was agreed that the model should be compared with experimental data from Berwick et al.

An interneuron is a specialised type of neuron whose primary role is to form a connection between other types of neurons. A large majority of interneurons of the central nervous system are of the inhibitory type. In contrast to excitatory neurons, inhibitory cortical interneurons characteristically release the neuro-transmitter GABA [9].

GABA is the main inhibitory neurotransmitter in the mammalian cortex [20]. Every third chemical synapse in the brain uses neurotransmitter GABA as an integral part of the neurotransmission process [21]. In $GABA_A$ receptors, binding of GABA molecules in the extracellular part of the receptor triggers the opening of a chlorine (Cl^-) ion selective pore, where the channel has a reversal potential of about -75 mV in neurons [3]. These receptors are also found on astrocytes [21] and smooth muscle [17].

Losi et al. [14] found that $GABA_A$ receptors on astrocytes are similar in many, though not all, aspects to those expressed

by neurons. One difference is that activation of astrocytic $GABA_A$ receptors leads to a depolarising current in mature astrocytes, as opposed to mature neurons, due to the $Na^+/K^+/Cl^-$ cotransporter (NKCC1) expression and activity that maintains a larger intracellular Cl^- concentration in astrocytes.

Anenberg et al. [2] found that optogenetic stimulation of GABAergic neurons (inhibitory interneurons) can lead to a net increase in cerebral blood flow (CBF). Whereas Uhlirova et al. [27] found that blood vessels in the brain will only constrict in response to inhibitory nerve cells. They identified NPY as a signal that triggers the constriction of the blood vessels. This signaling molecule is majorly expressed in interneurons and is released by a specific subtype of inhibitory nerve cell. NPY binds to a receptor protein on the SMCs and potentiates vasoconstriction by promoting Ca^{2+} entry into SMCs via voltage operated Ca^{2+} channels (VOCCs) [29, 31].

The neurotransmitter GABA (released in conjunction with NPY in inhibitory interneurons) mainly degrades to succinic semialdehyde and glutamate [25, 24]. This degradation is catalysed by the enzyme γ-aminobutyric acid transaminase (GABA-T), and increased GABA-T activity in the brain diminishes the GABA concentration [8]. Multiple experiments have shown that NO suppresses the activity of GABA-T and increases GABA, whereas a lack of NO (achieved through NO inhibitors such as N(ω)-nitro-L-arginine methyl ester (L-NAME)) increases GABA-T activity and reduces GABA concentration [8, 19, 26, 28].

In the experiments of Paul and Jayakumar [19] they found that the glutamate concentration stayed constant after administering L-NAME (and hence decreasing the NO concentration). They also found that the GABA concentration halved when L-NAME was introduced. The increase in GABA-T activity due to L-NAME is harder to determine due to the large variation in experiments, with increases ranging from 100% to 800% [28].

4.1 GABA and NPY pathways

A schematic of these two pathways is shown in Figure 15. The NPY pathway involves only the SMC. An increase in NPY concentration causes the VOCCs to open, allowing an influx of Ca^{2+} into the SMC leading to vasoconstriction [29, 31]. In contrast, the GABA pathway involves multiple cells and the primary effect is through GABA dependent Cl^- channels.

On the neuron, GABA opens Cl^- channels allowing an influx of Cl^- that hyperpolarises the neuron and inhibits any action potentials [23]. GABA also opens Cl^- channels on the astrocyte, allowing an efflux of chlorine from the astrocyte (the Cl^- travels out of the cell rather than inwards due to the NKCC1 cotransporter expression and activity that maintains a larger intracellular Cl^- concentration in astrocytes). Finally GABA opens Cl^- channels on the SMC, allowing an influx of Cl^- that hyperpolarises the SMC and closes the VOCCs; hence the Ca^{2+} concentration in the SMC decreases causing vasodilation [23].

GABA also degrades to glutamate in a reaction catalysed by the enzyme GABA-T (where GABA-T activity is inhibited by NO) [24]. Glutamate increases neuronal NO synthase (nNOS) production in the neuron which increases NO concentration and leads to vasodilation (note that the dynamics are slow and NO only has a minor effect over short time periods). Glutamate also leads to an increase in astrocytic inositol trisphosphate (IP_3) concentration via receptors on the astrocytic process. IP_3 causes a release of Ca^{2+} from internal stores leading to an increase in astrocytic Ca^{2+} and arachidonic acid (AA). The AA diffuses to the SMC and increases 20- hydroxyeicosatetraenoic acid (20-HETE) concentration which closes the big potassium (BK) channel. This leads to cell depolarisation, opening the VOCCs and leading to vasoconstriction.

4.2 Interneuron Model

In order to model these two pathways we use the NVU model as a base. A schematic of the previous excitatory neuron model is shown in Figure 1 whereas the new interneuron model is shown in Figure 16. The GABA and NPY

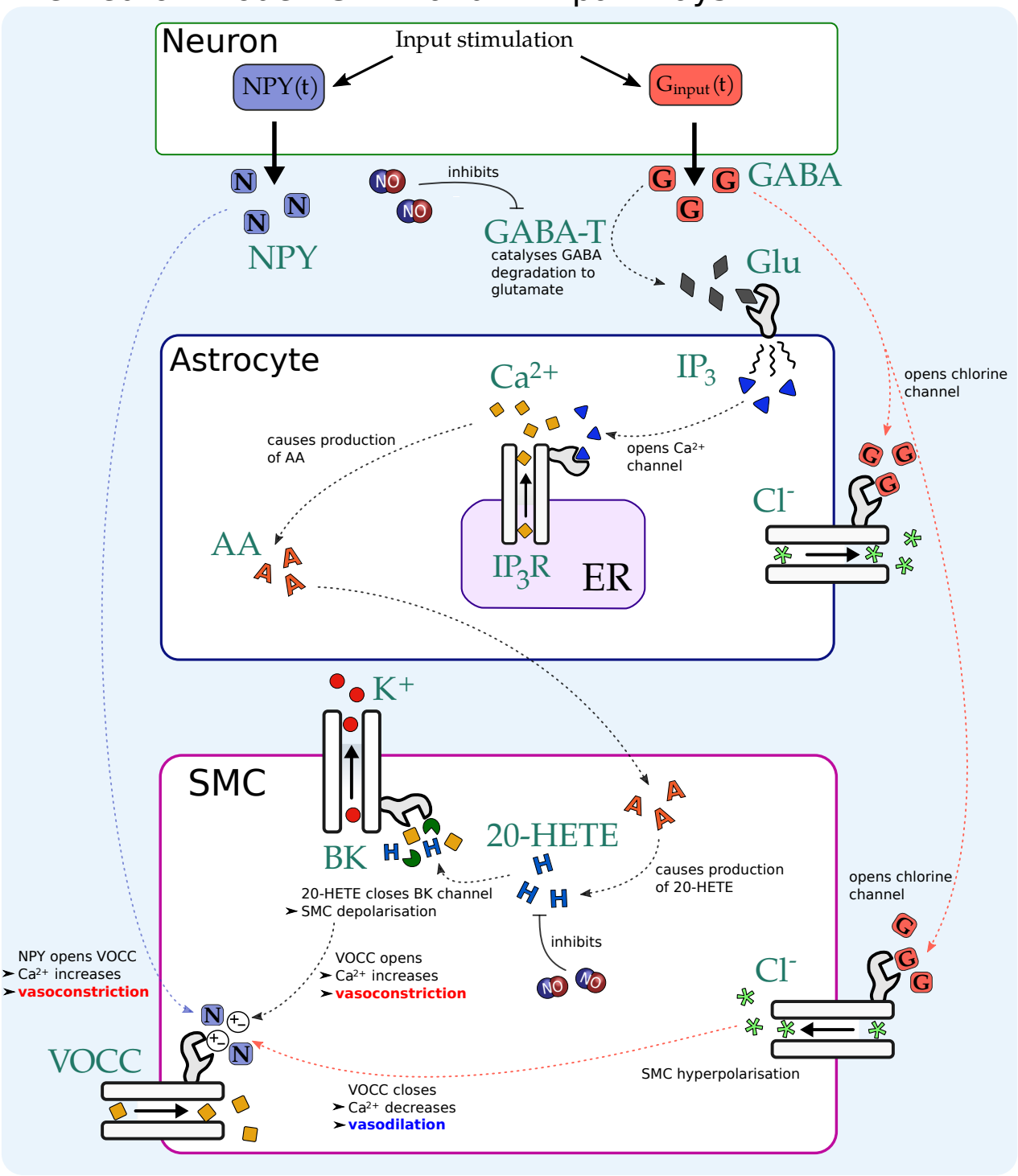

Figure 15: Schematic diagram of the GABA and NPY pathways in an interneuron model. Neuronal stimulation causes a release of NPY and GABA from the neuron. NPY opens the VOCC causing vasoconstriction. GABA opens Cl^- channels on the SMC causing cell hyperpolarisation and hence closes the VOCC leading to vasodilation. GABA also degrades to glutamate leading to an increase in astrocytic Ca^{2+} and AA. The AA diffuses to the SMC and increases 20-HETE concentration which closes the BK channel. This leads to cell depolarisation, opening the VOCC and leading to vasoconstriction.

concentrations are time dependent input functions that can be switched on or off as needed, where during stimulation the concentrations go from zero to some maximal value. The GABA concentration is determined with an ODE that is comprised of a degradation term (proportional to GABA-T activity) and a time dependent input simulating GABA release from the neuron during neuronal stimulation. The GABA-T activity is modelled as a sigmoid function that decreases with neuronal NO concentration.

The glutamate concentration is determined with an ODE and increases either due to vesicle release from an excitatory neuron or due to the degradation of GABA in an inhibitory neuron.

Two GABA dependent Cl^- channels are added, with one on the astrocyte and one on the SMC. These channels have a reversal potential of -75 mV and a channel conductance dependent on GABA; when GABA $= 0$, conductance $= 0$ and when GABA is at some maximal value, the conductance is also some maximal value G_{GABA}. At the moment this maximum is taken as $G_{GABA} = 0.3 \times G_{Cl,i}$ where $G_{Cl,i}$ is the conductance of the SMC Cl^- leak channel (value chosen to fit with Berwick experimental data). There is no GABA dependent Cl^- channel on the neuron as we don't have a neuronal membrane potential or Cl^- equation. Neuronal inhibition is simply modelled by a lack of neuronal stimulation.

The conductance of the VOCC in the SMC is multiplied by a NPY dependent function such that when NPY$= 0$, the VOCC conductance g_{VOCC} is equal to the regular conductance $G_{Ca,i}$ of the VOCC, and when NPY is at some maximal value g_{VOCC} is equal to $1.05 \times G_{Ca,i}$ (value chosen to fit with Berwick experimental data).

Extra reference: Adamchik et al. [1] formed a 2 variable model of a homogeneous neural population describing the behaviour of interneurons with tonic GABA conductance under the action of non-stationary ambient GABA (however they focused on the emergence of relaxation oscillations).

4.3 Interneuron model equations and parameters

The equations are given below and the parameters can be found in Table 1.

4.4 GABA

The model parameters used in the following equations are chosen to fit with the experimental findings of Paul and Jayakumar [19] and Vega Rasgado et al. [28] so that when L-NAME is administered we obtain a decrease of 50% in GABA concentration and increase of 100% in GABA-T activity.

The GABA concentration is nondimensionalised with respect to some maximal value so that at rest the concentration is zero and during regular neuronal stimulation the nondimensional concentration $GABA_N$ is 1. The ODE for $GABA_N$ is given by

$$\frac{dGABA_N}{dt} = -\kappa_{GABA}\, GABA_N + G_{input}(t) \tag{26}$$

where the first term on the RHS models GABA degradation and $G_{input}(t)$ is a time dependent input function simulating an input of GABA during neuronal stimulation modelled via a heaviside function:

$$G_{input}(t) = \begin{cases} 1 & t_0 < t < t_0 + \Delta t \\ 0 & \text{otherwise} \end{cases} \tag{27}$$

where t_0 is the beginning of stimulation and Δt is the length of stimulation. The rate at which GABA degrades is given by κ_{GABA} and is proportional to the GABA-T activity $(G_{T,act})$, where GABA-T is the enzyme that catalyses the

Interneuron model

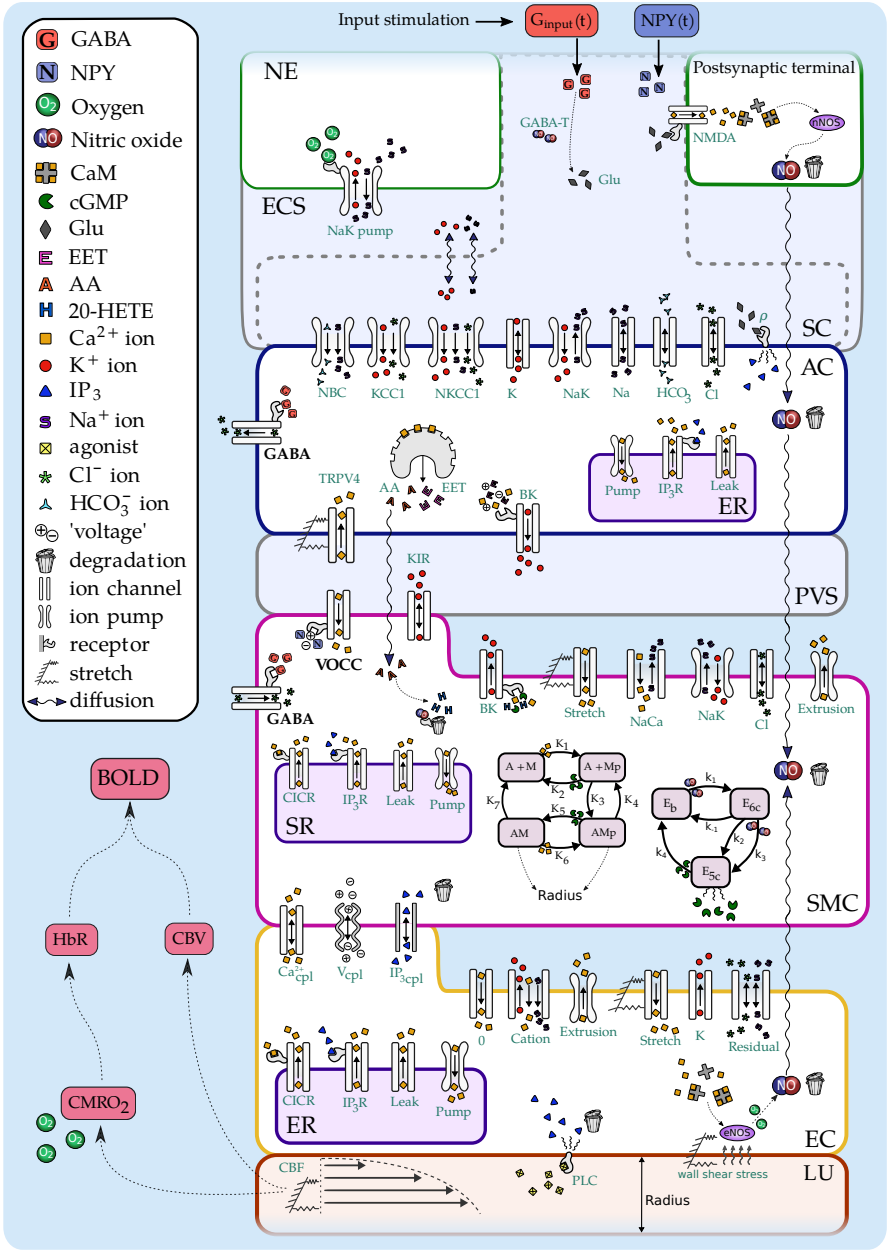

Figure 16: Interneuron model (compare with Figure 1)

degradation reaction:

$$\kappa_{GABA} = p_1 G_{T,act} \tag{28}$$

where $p_1 = 1\ \mathrm{s}^{-1}$ is a scaling parameter to obtain the correct units (s^{-1}). The GABA-T activity is inhibited via NO and modelled with sigmoidal function:

$$G_{T,act} = G_{T,min} + (G_{T,max} - G_{T,min}) \frac{1}{1 + \left[\left(\frac{NO_i - NO_{rest}}{R_{NO}}\right)\right]} \tag{29}$$

where $G_{T,min} = 1$ is the minimum activity (i.e. when NO_n is at normal resting value, $NO_{rest} \approx 0.02047$ μM and $R_{NO} \approx 0.02\mu$M), $G_{T,max} = 2$ is the maximum activity (i.e. when $NO_n \approx 0$ μM), and $p_2 = 200$ $\mu\mathrm{M}^{-1}$ is a scaling parameter. Note that $G_{T,act}$ is nondimensional and normalised w.r.t. some minimal value.

The glutamate concentration can either be increased due to neuronal stimulation as in an excitatory neuron (modelled as a glutamate release when extracellular K^+ concentration K_e is above some threshold) or increased from the degradation of GABA in an inhibitory interneuron (as GABA degrades to succinic semialdehyde and glutamate when catalysed by GABA-T). The nondimensional glutamate concentration Glu (normalised w.r.t. some maximal value) is modelled by the following equation:

$$\frac{dGlu}{dt} = f(K_e) + g(GABA) - p_1\, Glu \tag{30}$$

where $f(K_e)$ is a function that models the neuronal release of glutamate and $f(GABA)$ is a function that models the production of glutamate from the degradation of GABA. These two functions are given by

$$f(K_e) = \frac{p_1}{2}\left(1 + \tanh\left[\frac{K_e - Ke_{switch}}{Glu_{slope}}\right]\right) \tag{31}$$

where $Ke_{switch} = 5$ mM is the concentration above which glutamate is released from the neuron and $Glu_{slope} = 0.1$ mM is the slope of the sigmoidal (both parameters taken from the previous version of the model [15]), and

$$g(GABA) = \kappa_{GABA}\, GABA \tag{32}$$

where κ_{GABA} is the degradation rate of GABA (see Equation 28). At rest both $f(K_e)$ and $f(GABA)$ are zero and so the glutamate concentration tends to zero.

The GABA dependent Cl^- channel fluxes on the astrocyte and SMC are added to the differential equations for v_k and v_i respectively and are given by

$$J_{GABA,k} = g_{GABA}(v_k - E_{GABA}) \tag{33}$$

$$J_{GABA,i} = g_{GABA}(v_i - E_{GABA}) \tag{34}$$

where v_k is the astrocytic membrane potential in mV, v_i is the SMC membrane potential in mV, $E_{GABA} = -75$ mV is the reversal potential of the Cl^- channels, and the GABA dependent conductance of the channels is given by

$$g_{GABA} = \frac{G_{GABA}}{2}\left(1 + \tanh\left(\frac{GABA_N - g_{mid}}{g_{slope}}\right)\right) \tag{35}$$

where $g_{mid} = 0.8$ is the midpoint of the sigmoidal, g_{slope} is the slope of the sigmoidal (both model estimates), and G_{GABA} is the maximal conductance of the channel given by $0.3 \times G_{Cl,i}$ where $G_{Cl,i} = 1.34 \times 10^{-6}$ μM mV^{-1} ms^{-1} is the conductance of the SMC Cl^- leak channel taken from the NVU model. This is a model estimate and can be changed by fitting to data. Hence when $GABA_N = 0$, $g_{GABA} = 0$ and when $GABA_N = 1$, $g_{GABA} = G_{GABA}$.

4.5 NPY

NPY is given by a time dependent input function (heaviside function):

$$NPY_N(t) = \begin{cases} 1 & t_0 < t < t_0 + \Delta t \\ 0 & \text{otherwise} \end{cases} \tag{36}$$

where t_0 is the beginning of stimulation and Δt is the length of stimulation. Note that the NPY concentration is nondimensionalised with respect to its maximal value (currently unknown), i.e. $NPY_N = NPY/NPY_{max}$ so that during the stimulation period $NPY_N = NPY_{max}/NPY_{max} = 1$.

Finally the flux of Ca^{2+} through the VOCC channel on the SMC is given by

$$J_{VOCC,i} = g_{VOCC} \frac{v_i - v_{Ca1}}{1 + \exp\left(\frac{-(v_i - v_{Ca2})}{R_{Ca}}\right)} \tag{37}$$

where $v_{Ca1} = 100$ mV is the reversal potential, $v_{Ca2} = -24$ mV is the half-point of the VOCC activation sigmoidal, and $R_{Ca} = 8.5$ mV is the maximum slope of the sigmoidal (all taken from the NVU model). The NPY conductance is given by

$$g_{VOCC} = G_{Ca,i}\left(1 + \frac{N_{inc}}{2}\tanh\left(\frac{NPY_N - N_{mid}}{N_{slope}}\right)\right) \tag{38}$$

where $G_{Ca,i} = 1.29 \times 10^{-6}$ μM mV^{-1} ms^{-1} is the base conductance of the VOCC (taken from the NVU model), $N_{inc} = 0.05$ is the proportional increase of the conductance from baseline due to NPY (i.e. 0.05 means a 5% increase from $G_{Ca,i}$ when NPY is released, model estimate), $N_{mid} = 0.6$ is the midpoint of the sigmoidal, and $N_{slope} = 0.1$ is the slope of the sigmoidal (both model estimates). Hence when $NPY_N = 0$, $g_{VOCC} = G_{Ca,i}$ and when $NPY_N = 1$, $g_{VOCC} = 1.05 \times G_{Ca,i}$.

Parameter	Description	Value	Reference
p_1	Scaling parameter for unit conversion	1 s^{-1}	
$G_{T,min}$	Minimum GABA-T activity	1	[28]
$G_{T,max}$	Maximum GABA-T activity	2	[28]
E_{GABA}	Reversal potential of the GABA dependent Cl^- channels	-75 mV	[3]
G_{GABA}	Conductance of GABA dependent Cl^- channel	4.02×10^{-7} μM mV^{-1} ms^{-1}	[12]
g_{mid}	Midpoint of the g_{GABA} sigmoidal	0.8	M. E.
g_{slope}	Slope of the g_{GABA} sigmoidal	0.1	M. E.
N_{inc}	proportional increase in VOCC conductance due to NPY	0.05	M. E.
N_{mid}	Midpoint of the g_{VOCC} sigmoidal	0.6	M. E.
N_{slope}	Slope of the g_{VOCC} sigmoidal	0.1	M. E.

Table 1: New parameters of the GABA and NPY model.

We should note that version 3.3 now includes the GABA and NPY pathways as part of the somatosensory cortex

simulations and is a function of the inhibitory output I(t).

$$\begin{aligned}
\frac{dGABA}{dt} &= -\kappa_{GABA} * (GABA - GABA_{base}) + \alpha_{GABA} \frac{(I_t - I_{min})}{(I_{relative} - I_{min})} \\
\frac{dNPY}{dt} &= -\beta_{NPY}(NPY - NPY_{base}) + \alpha_{NPY} \frac{(I_t - I_{min})}{(I_{relative} - I_{min})} \\
\frac{dGlu}{dt} &= -\beta_{Glu} Glu + Glu_{Switch}(f(K_e) + g(GABA)) \\
f(K_e) &= \frac{\beta_{Glu}}{2}\left[1 + tanh\left(\frac{K_e - K_{e,switch}}{Glu_{slope}}\right)\right] \\
g(GABA) &= \kappa_{GABA} GABA
\end{aligned} \tag{39}$$

here is an inconsistency here as β_{Glu} cannot be both s^{-1} and $\mu\text{M}s^{-1}$ since Glu_{switch} is non-dimensional

This allows investigation into the influence (or otherwise) of GABA and NPY during "normal" somatosensory coretx stimulation. We do not yet have any experimental evidence that this actually occurs.

Parameter	Description	Value
α_{GABA}		2.6×10^{-3} μM
β_{GABA}		4.2×10^{-3} s^{-1}
α_{NPY}		2.6×10^{-3} μM
β_{NPY}		4.2×10^{-3} s^{-1}
β_{Glu}		4.2×10^{-3} s^{-1}
$K_{e,switch}$		5.0 mM
Glu_{slope}		0.1 mM
$GABA_{base}$		0.0 μM
NPY_{base}		0.0 μM
I_{min}		0.225 These depend on whether the model uses thalamic or somatosonsory input
$I_{relative}$		1.512 as above

5 Equations and Parameters for the Full NVU Model

The following parameters are given for ordinary neurovascular coupling (NVC) conditions.

Parameter	Description	Value
F	Faraday's constant	96.485 C mmol^{-1}
R_g	Gas constant	8.315 J mol^{-1} K^{-1}
T	Temperature constant	300 K
ϕ	R_gT/F characteristic voltage	26.7 mV
z_K	Ionic valence for K^+	1
z_{Na}	Ionic valence for Na^+	1
z_{Cl}	Ionic valence for Cl^-	-1
z_{NBC}	Effective valence of the NBC cotransporter complex	-1
z_{Ca}	Ionic valence for Ca^{2+}	2
γ_v	Change in membrane potential by a scaling factor	1970 mV μM $^{-1}$

5.1 Some Notes on Basic Hematology

In order to properly compare with some of the experimental results from both Sheffield (Jason Berwick's group) and others we look at some parameters corresponding to hæmoglobin dynamics.
hæmoglobin concentration in blood

- Adult Male :- 135-175 gL^{-1}
- Adult Female :- 122-150 gL^{-1}
- Child :- 100-140 gL^{-1}

Molecular weight of hæmoglobin = 64450 $gmol^{-1}$.

- Adult Male :- 2.1-2.7 mM
- adult Female :- 1.9-2.3 mM Child :- 1.55-2.2 mM

hæmoglobin , [H] decreases from the large arteries to the cerebral vasculature in a ratio of 0.69 (see Wyatt et al 1990, Jour Appli., Physiology, **68**, 1086-1091). With [H]= 2.5 mM in aorta then $[H]_{brain} = [H]_b = 2.5 \times 0.69 = 1.725mM$. Using the Hill equation and a blood saturation of 0.75 we have that

$$[O_2]b = [O_2]_{plasma} + \frac{[H]bPO}{1 + \frac{\alpha P_{50}}{[O_2]_{plasma}}} \tag{40}$$

$P_{50} = P_{O_2}$ at which [H] is 50 % saturated.
(see Valabrague et al , JCBFM, **23**:536-545, 2003). Solving the Hilll equation for $[O_2]_{plasma} = 0.053mM$.
(See Hudetz, 1999, Brain Res. **817**:75-83) the ratio of oxygnen concentration in cerebral tissue to plasma is approximately 0.2 = g.

- Average normal CBV: 3.5 %
- Gray Matter : 4.7 %
- White Matter : 2.6 %
- Basal Ganglia : 3.9 %

Hence

- $[HbT]_{tissue} = 1.725mM \times 3.5\% = 60\mu M.$
- Gray Matter $[HbT]_{tissue} = 1.725mM \times 4.7\% = 82\mu M.$
- Assume $[HbT]_{tissue} = 75\mu M.$

Here we use the formulation of Buxton for CMRO2 as the definitions seem to be non-aligned. CMRO2 is NOT the rate at which the neuron consumes O2 but the product of the flow in the capillary, the oxygen extraction fraction and the basal oxygen concentration in the precapillary arteriole. In addition the flux J_{vasc} is now formed from the oxygen extraction fraction, CBF and the basal oxygen concentration. We define below the new extraction fraction using the analysis of Buxton and Frank and use this in the equations for HbR etc.

Extraction fraction
Assumptions

- At rest all brain capillaries are perfused. No capillary recruitment
- All O2 leaving the capillary are used by the cell's metabolism. i.e. 100 % efficiency
- exchange of O2 between plasma and RBCs is rapid and hence in equilibrium
- O2 has a probability k, of beinf extracted for metabolism. In the simple model k is proportional to the capillary wall permeability P.

Using the above asumptions then defining $C_p(t)$ as the plasma oxygen concentration, $C_T(t)$ the total oxygen concentraiton in the capillary then

$$\frac{dC_T(t)}{dt} = -kC_p(t) \tag{41}$$

with $C_T(0) = C_a$. The extraction fraction is defined as

$$E_t(t) = \frac{C_T(0) - C_T(t)}{C_T(0)} \tag{42}$$

Suppose that $r = \frac{C_p(t)}{C_T(t)} =$ constant and with all capillaries having the same transit time then the solution to equation (5.1) is ,

$$E = 1 - e^{rkt} \tag{43}$$

Assuming that the volume of the capillary bed remains constant then the characteristic time through the capillary bed is inversely proportional to the flow velocity, $f_{in} = f$.

$$\begin{aligned} E_0 &= 1 - e^{rk/f_0} \\ k &= \frac{ln(1 - E_0)^{f_0}}{r} \\ E(f) &= 1 - (1 - E_0)^{f_0/f} \end{aligned} \tag{44}$$

In this case f is defined to be cerebral blood flow, CBF. However the probability of oxygen crossing the BBB is proportional to the concentration gradient of oxygen in the plasma to that in the cerebral tissue = 0.2, hence we redevelop

the Buston extraction fraction equation to include this.

$$g = \frac{[O_2]_{tissue}}{[O_2]_{plasma}}$$
$$E(f) = 1 - (1 - E_0)^{\frac{f_0}{f(1-g)}} \tag{45}$$

In the model we use equation (5.1) since $E(f_{in})$ defined in equation (5.1) is not unity.

6 Neuron and Extracellular Space

For the simple neuron model we need to list the inputs to the astrocyte initially to ensure that all required ion concentrations are provided as time-dependent functions. The astrocyte requires concentrations of

- Glutamate
- K^+
- Na^+
- HCO_3^-
- Cl^-

6.1 Input to the model

The input to the neuron model is in two parts. Firstly that of the activation of excitatory neurons (E(t)) defined as P(t) and secondly the activation of inhibitory neurons (I(t)) defined as Q(t). These are given in the first case as rectangular functions.

$$P(t) = \begin{cases} P_{strength} & \text{for } t_0 \leq t \leq t_f \\ 0 & otherwise \end{cases} \tag{46}$$

and

$$Q(t) = \begin{cases} Q_{strength} & \text{for } t_0 \leq t \leq t_f \\ 0 & otherwise \end{cases} \tag{47}$$

6.2 ODEs

see Table 6.3 for parameter definitions Excitatory (E(t)) and Inhibitory (I(t)) non-dimensional functions :

$$\frac{dE}{dt} = \frac{1}{\tau_E}\left\{-E(t) + (k_e - r_e E(t))S_e(c_1 E(t) - c_2 I(t) + P(t))\right\} \tag{48}$$
$$\frac{dI}{dt} = \frac{1}{\tau_I}\left\{-I(t) + (k_i - r_i I(t))S_i(c_3 E(t) - c_4 I(t) + Q(t))\right\} \tag{49}$$

here the functions S_e and S_i are given by

$$S_n(x) = \frac{1}{1 + exp\left[-a_n(x - \theta_n)\right]} - \frac{1}{1 + exp(a_n\theta_n)} \quad n \in e, i \tag{50}$$

with

$$k_n = max\left[S_n(x)\right] \quad n \in e, i \tag{51}$$

Table 6.3

Parameter	Description	Value
a_e	sigmoid coefficient	1.2
θ_e	sigmoid coefficient	2.8
τ_e	characteristic time for excitatory neurons	3 ms
a_i	sigmoid coefficient	1.0
θ_i	sigmoid coefficient	4.0
τ_1	characteristic time for inhibitory neurons	3 ms
r_e	coefficient	1
r_i	coefficient	1
c_1	coefficient	12
c_2	coefficient	10
c_3	coefficient	13
c_4	coefficient	11

Table 4: Nominal parameters of the neuron populations.

We should note here that the nominal parameters given in Table 6.3 could change depending on the experimental stimulation. This variation has yet to be fully investigated and described. To find the value of $k_{e,i}$ we use x = 10 such that $k_n = S_n(x)$ and this gives a good approximation to the maximum value.

The Na^+ ion concentrations in the soma and dendrite and theK^+ in the extracellular space (ECS) respectively (mM):

$$\frac{dNa_{sa}}{dt} = -\beta_{Na_{sa}}(Na_{sa} - Na_{sabase}) + \alpha_{Na_{sa}}\beta_{Na_{sa}}\frac{[\mid E(t) - I(t) \mid]}{EI_0} \tag{52}$$

$$\frac{dNa_d}{dt} = -\beta_{Na_d}(Na_d - Na_{dbase}) + \alpha_{Na_d}\beta_{Na_d}\frac{[\mid E(t) - I(t) \mid]}{EI_0} \tag{53}$$

$$\frac{dK_e}{dt} = -\beta_{Ke}(K_e - K_{base}) + \alpha_{Ke}\beta_{Ke}\frac{[\mid E(t) - I(t) \mid]}{EI_0} \tag{54}$$

Table 6.2

Parameter	Description	Value
α_{Ke}		2.1 (this can vary)
β_{Ke}		4.2e-3
$\alpha_{Na_{sa}}$		4.23
$\beta_{Na_{sa}}$		0.39e-3
α_{Na_d}		-2.12
β_{Na_d}		0.75e-3
K_{base}		3.5
Na_{sabase}		9.37
Na_{dbase}		9.42

Table 5: Nominal parameters of the neuron populations.

Again we should note here that the nominal parameters given in Table 6.2 could change depending on the experimental stimulation. This variation has yet to be fully investigated and described.

The oxygen consumption ode is the same as the old Kager neuron model.

$$\frac{dO_2}{dt} = J_{O_{2_{vascular}}} - J_{O_{2_{background}}} - J_{O_{2_{pump}}} \tag{55}$$

In the full model this PUMP is defined as $J_{O_{2pump}}$ which is function of the ECS K^+ and the soma or dendrite concentration of Na^+. This works for the new model as all we need to know is the concentrations of ECS K^+ and the soma or dendrite concentration of Na^+ and we have that from the solution of the 'simple' odes.

The cerebral blood flow (-):(assuming Poiseuille Flow)

$$\text{CBF} = \text{CBF}_{init}\frac{R^4}{R^4_{init}} \tag{56}$$

6.3 Algebraic Variables

The vascular supply of oxygen (mM s^{-1}) is defined by the amount of oxygen extracted and passed across the blood brain barrier, since CBF is defined in terms of mMs^{-1}:

$$J_{O_2\ vascular} = CBF\frac{E(t)}{E_0} \tag{57}$$

Note here that E(t) is NOT the excitatory neuron function but the Extraction fraction as given in section 5.1 !
The background oxygen consumption (mM s^{-1}):

$$J_{O_2\ background} = J_0 P_{O2}(1 - \gamma_{O2}) \tag{58}$$

The normalised pump rateP_{O2}(-):

$$P_{O2} = \frac{J_{pump2}(O2) - J_{pump2}(0)}{J_{pump2}(O2_o) - J_{pump2}(0)} \tag{59}$$

We can simplify this considerably since

$$\begin{aligned} J_{pump2}(O2) &= 2\left[1 + \frac{O2_o}{(1-\alpha_{O2})O2 + \alpha_{O2}O2_o}\right]^{-1} \\ J_{pump2}(O2_o) &= 1 \\ J_{pump2}(0) &= 2\left[1 + \frac{1}{\alpha_{O2}}\right]^{-1} = \frac{2\alpha_{O2}}{1+\alpha_{O2}} \end{aligned} \tag{60}$$

so

$$\begin{aligned} J_{pump2}(O2_o) - J_{pump2}(0) &= 1 - \frac{2\alpha_{O2}}{1+\alpha_{O2}} \\ &= \frac{1-\alpha_{O2}}{1+\alpha_{O2}} \end{aligned} \tag{61}$$

hence the nomalised pump rate is evaluated as

$$\begin{aligned} P_{O2} &= \frac{J_{pump2}(O2) - \frac{2\alpha_{O2}}{1+\alpha_{O2}}}{\frac{1-\alpha_{O2}}{1+\alpha_{O2}}} \\ &= \frac{(1+\alpha_{O2})J_{pump2}(O2) - 2\alpha_{O2}}{1-\alpha_{O2}} \end{aligned} \tag{62}$$

finally we have the reduction of oxygen due to the ATP-ase pump in the neuron.

$$\begin{aligned} J_{O_{2_{pump}}} &= J_0 P_{0_2} \gamma_{O_2} \frac{((J_{pump1_{sa}} + J_{pump1_d})}{(J_{pump1init_{sa}} + J_{pump1init_d}))} \\ J_{pump1_{sa}} &= \left(1 + \left(\frac{K_{e,0}}{K_e}\right)\right)^{-2} \left(1 + \frac{Na_{sa,0}}{Na_{sa}}\right)^{-3} \\ J_{pump1init_{sa}} &= 0.0312 \\ J_{pump1_d} &= \left(1 + \left(\frac{K_{e,0}}{K_e}\right)\right)^{-2} \left(1 + \left(\frac{Na_{d,0}}{Na_d}\right)\right)^{-3} \\ J_{pump1init_d} &= 0.0312 \end{aligned} \tag{63}$$

Parameter	Description	Value
t_0	Start time of input current	0 s
t_f	Final time of input current	variable
$O2_0$	Equilibrium tissue oxygen level	0.01 mM
γ_{O2}	Fraction of the total oxygen consumption at steady state	0.1
J_0	Equilibrium change in oxygen concentration due to CBF	0.053 mM s^{-1}
CBF_{init}	Equilibrium CBF	0.032
$J_{pump1_{sa_0}}$	Steady state pump rate in the soma/axon	0.0312
$J_{pump1_{d_0}}$	Steady state pump rate in the dendrite	0.0312
R_{init}	Vessel radius when passive and no stress is applied	20 μm
α_{O2}	Fraction of oxygen independent adenosine triphosphate (ATP) production	0.05
$J_{pump2}(0)$	Pump rate when oxygen concentration is 0	0.0952
$J_{pump2}(O2_0)$	Pump rate when oxygen is at equilibrium	1
$K_{e,0}$	Equilibrium K_e	2.9 mM
$Na_{sa,0}$	Equilibrium Na_{sa}	10 mM
$Na_{d,0}$	Equilibrium Na_d	10 mM
I_{max}	Maximum rate of Na^+/K^+ ATP-ase pump	0.078 mA cm^{-2}

Table 6: Parameters of the neuron and extracellular space submodel, for references see Mathias et al. [16].

7 Synaptic Cleft and Astrocyte

7.1 ODEs

Note that GABA and NPY related equation components are denoted in red for clarity.

K^+ concentration in the synaptic cleft (SC) (μM):

$$\frac{dK_s}{dt} = \frac{1}{VR_{sk}} \left(J_{K_k} - 2J_{NaK_k} - J_{NKCC1_k} - J_{KCC1_k}\right) + J_{KNEtoSC} \tag{64}$$

Na^+ concentration in the SC (μM):

$$\frac{dNa_s}{dt} = \frac{1}{VR_{sk}} \left(J_{Na_k} + 3 * J_{NaK_k} - J_{NKCC1_k} - J_{NBC_k}\right) - J_{NaNEtoSC} \tag{65}$$

HCO_3^- concentration in the SC (μM):

$$\frac{dHCO_{3_s}}{dt} = \frac{1}{VR_{sk}} \left(-2J_{NBC_k}\right) \tag{66}$$

K^+ concentration in the astrocyte (μM):

$$\frac{dK_k}{dt} = -J_{K_k} + 2J_{NaK_k} + J_{NKCC1_k} + J_{KCC1_k} - J_{BK_k} \tag{67}$$

Na^+ concentration in the astrocyte (μM):

$$\frac{dNa_k}{dt} = -J_{Na_k} - 3J_{NaK_k} + J_{NKCC1_k} + J_{NBC_k} \tag{68}$$

HCO_3^- concentration in the astrocyte (μM):

$$\frac{dHCO_{3_k}}{dt} = 2J_{NBC_k} \tag{69}$$

Cl^- concentration in the astrocyte via electroneutrality (μM):

$$\frac{dCl_k}{dt} = \frac{dNa_k}{dt} + \frac{dK_k}{dt} - \frac{dHCO_{3_k}}{dt} + 2\frac{dCa_k}{dt} \tag{70}$$

The astrocytic cytosolic Ca^{2+} concentration (μM):

$$\frac{dCa_k}{dt} = B_{cyt}\left(J_{IP3_k} - J_{pump_k} + J_{ERleak_k} - \frac{J_{TRPV_k}}{r_{buff}} + J_{CICR_k}\right) \tag{71}$$

note that the astrocyte now has a CICR flux which Figure 16 doesn't show

The astrocytic IP_3 concentration (μM):

$$\frac{dIP3_k}{dt} = r_h G - k_{deg}\, IP3_k \tag{72}$$

The astrocytic epoxyeicosatrienoic acid (EET) concentration (μM):

$$\frac{deet_k}{dt} = V_{eet}\max(Ca_k - c_{k_{min}}, 0) - k_{eet}eet_k \tag{73}$$

The Ca^{2+} concentration in the astrocytic endoplasmic reticulum (ER) (μM):

$$\frac{ds_k}{dt} = \frac{-B_{cyt}}{VR_{ERcyt}}\left(J_{IP3_k} - J_{pump_k} + J_{ERleak_k} + J_{CICR_k}\right) \tag{74}$$

Membrane potential of the astrocyte (AC) (mV):

$$\frac{dv_k}{dt} = \gamma_v(-J_{BK_k} - J_{K_k} - J_{Cl_k} - J_{NBC_k} - J_{Na_k} - J_{NaK_k} - 2J_{TRPV_k} - J_{GABA,k}) \tag{75}$$

The open probability of the BK channel (-):

$$\frac{dw_k}{dt} = \phi_n(w_\infty - w_k) \tag{76}$$

The inactivation variable h_k of the astrocytic IP_3R channel (-):

$$\frac{dh_k}{dt} = k_{on}\left[K_{inh} - (Ca_k + K_{inh})h_k\right] \tag{77}$$

The TRPV4 channel open probability

$$\frac{dm_k}{dt} = trpv4switch\frac{(m_{inf} - m_k)}{\tau_{TRPV4}} \tag{78}$$

The concentration of arachidonic acid in the astrocyte AA_k.

$$\frac{dAA_k}{det} = \frac{AA_m AA_{max}}{(AA_m + (Ca_k - Ca_0))^2 \frac{dCa_k}{dt}} + \frac{(AA_i - AA_k)}{\tau_{AA}} \tag{79}$$

$$\tau_{AA} = \frac{x_{ki}^2}{2D_{AA}} \tag{80}$$

7.2 Algebraic Variables

The glutamate concentration in the SC (μM):

$$Glu = \frac{Glu_{max}}{2}\left(1+\tanh\left(\frac{K_e - Ke_{switch}}{Glu_{slope}}\right)\right) + \frac{Glu_{max}}{2}\left(1+\tanh\left(\frac{GABA_N - g_{mid}}{g_{slope}}\right)\right) \tag{81}$$

$$J_{GABA,k} = g_{GABA}(v_k - E_{GABA}) \tag{82}$$

$$g_{GABA} = \frac{G_{GABA}}{2}\left(1+\tanh\left(\frac{GABA_N - g_{mid}}{g_{slope}}\right)\right) \tag{83}$$

G_{GABA} is the maximal conductance of the channel given by $0.3 \times G_{Cl,i}$ where $G_{Cl,i} = 1.34 \times 10^{-6}$ μM mV^{-1} ms^{-1} is the conductance of the SMC Cl^- leak channel taken from the excitatory NVU model (i.e. Wilson Cowan).

The flux of K^+ into the SC based on the extracellular K^+ (μMs^{-1}):

$$J_{KNEtoSC} = J_{NaNEtoSC} = c_{unit} k_{syn} \frac{dK_e}{dt} \tag{84}$$

Cl^- concentration in the SC via electroneutrality (μM):

$$Cl_s = Na_s + K_s - HCO3_s \tag{85}$$

Cl^- flux through the Cl^- channel (μM s^{-1}):

$$J_{Cl_k} = G_{Cl_k}(v_k - E_{Cl_k}) \tag{86}$$

K^+ flux through the K^+ channel (μM s^{-1}):

$$J_{K_k} = G_{K_k}(v_k - E_{K_k}) \tag{87}$$

Na^+ flux through the Na^+ channel (μM s^{-1}):

$$J_{Na_k} = G_{Na_k}(v_k - E_{Na_k}) \tag{88}$$

Na^+ and HCO_3^- flux through the NBC channel (μM s^{-1}):

$$J_{NBC_k} = G_{NBC_k}\,(v_k - E_{NBC_k}) \tag{89}$$

Cl^- and K^+ flux through the KCC1 channel (μM s^{-1}):

$$J_{KCC1_k} = G_{KCC1_k}\phi \ln\left(\frac{K_s Cl_s}{K_k Cl_k}\right) \tag{90}$$

Na^+, K^+ and Cl^- flux through the NKCC1 channel (μM s^{-1}):

$$J_{NKCC1_k} = G_{NKCC1_k}\phi \ln\left(\frac{Na_s K_s {Cl_s}^2}{Na_k K_k {Cl_k}^2}\right) \tag{91}$$

Flux through the Na^+/K^+ ATP-ase pump (μM s^{-1}):

$$J_{NaK_k} = J_{NaK_{max}} \frac{{Na_k}^{1.5}}{{Na_k}^{1.5} + {K_{Na_k}}^{1.5}} \frac{K_s}{K_s + K_{K_s}} \tag{92}$$

K^+ flux through the BK channel (μM s^{-1}):

$$J_{BK_k} = G_{BK_k} w_k\,(v_k - E_{BK_k}) \tag{93}$$

Nernst potential for the K^+ channel (mV):

$$E_{K_k} = \frac{\phi}{z_K} \ln\left(\frac{K_s}{K_k}\right) \tag{94}$$

Nernst potential for the Na^+ channel (mV):

$$E_{Na_k} = \frac{\phi}{z_{Na}} \ln\left(\frac{Na_s}{Na_k}\right) \tag{95}$$

Nernst potential for the Cl^- channel (mV):

$$E_{Cl_k} = \frac{\phi}{z_{Cl}} \ln\left(\frac{Cl_s}{Cl_k}\right) \tag{96}$$

Nernst potential for the NBC channel (mV):

$$E_{NBC_k} = \frac{\phi}{z_{NBC}} \ln\left(\frac{Na_s {HCO_3}_s^2}{Na_k {HCO_3}_k^2}\right) \tag{97}$$

Nernst potentical for TRPV4 channel (mV):

$$E_{TRPV_k} = \frac{\phi}{z_{Ca}} ln\left(\frac{Ca_p}{Ca_k}\right) \tag{98}$$

Nernst potential for the BK channel (mV):

$$E_{BK_k} = \frac{\phi}{z_K} \ln\left(\frac{K_p}{K_k}\right) \tag{99}$$

The time constant associated with the opening of the BK channel (s^{-1}):

$$\phi_n = \psi_n \cosh\left(\frac{v_k - v_3}{2v_4}\right) \tag{100}$$

The equilibrium state of the BK channel (-):

$$w_\infty = \frac{1}{2}\left(1 + \tanh\left(\frac{v_k + eet_{shift}eet_k - v_3}{v_4}\right)\right) \tag{101}$$

The voltage associated with half open probability (mV):

$$v_3 = -\frac{v_5}{2} \tanh\left(\frac{Ca_k - Ca_3}{Ca_4}\right) + v_6 \tag{102}$$

The ratio ρ of bound to unbound metabotropic receptors on the astrocytic process adjacent to the SC (-):

$$\rho = \rho_{\text{min}} + \frac{\rho_{\text{max}} - \rho_{\text{min}}}{Glu_{max}} Glu \tag{103}$$

The ratio G of active to total G-protein due to metabotropic glutamate receptor (mGluR) binding on the astrocyte endfoot surround the SC (-):

$$G = \frac{\rho + \delta_G}{K_G + \rho + \delta_G} \tag{104}$$

Fast Ca^{2+} buffering in the astrocytic cytosol is described within the steady state approximation (-):

$$B_{cyt} = \left(1 + BK_{end} + \frac{K_{ex}B_{ex}}{(K_{ex} + Ca_k)^2}\right)^{-1} \tag{105}$$

The flux of Ca^{2+} through the IP_3R channel (μM s^{-1}):

$$J_{IP3_k} = J_{max}\left[\left(\frac{IP3_k}{IP3_k + K_i}\right)\left(\frac{Ca_k}{Ca_k + K_{act_k}}\right)h_k\right]^3 \left(1 - \frac{Ca_k}{s_k}\right) \tag{106}$$

The flux of Ca^{2+} through the uptake pump (μM s^{-1}):

$$J_{pump_k} = V_{max} \frac{Ca_k^2}{Ca_k^2 + k_{pump}^2} \tag{107}$$

The flux of Ca^{2+} through the leak channel (μM s^{-1}):

$$J_{ERleak_k} = P_L \left(1 - \frac{Ca_k}{s_k}\right) \tag{108}$$

flux of Ca^{2+} through CICR into astrocytic cytosol

$$J_{CICR_k} = C_k * \frac{s_k^4}{sc_k^4 + s_k^4} \frac{Ca_k^4}{cc_k^4 + Ca_k^4} \tag{109}$$

flux of Ca^{2+} through TRPV4 channel

$$J_{TRPV_k} = G_{TRPV_k} m_k (v_k - E_{TRPV_k}) \tag{110}$$

Parameter	Description	Value
VR_{sk}	Volume ratio between the SC and astrocyte	0.465
Glu_{max}	Maximum glutamate concentration (one vesicle)	1846 μM
$K_{e_{switch}}$	Threshold past which glutamate is released	5.0 mM
Glu_{slope}	Slope of glutamate sigmoidal	0.1 mM
c_{unit}	Constant to convert from mM to μM	10^3
k_{syn}	The number of active synapses per astrocytic process	11.5
G_{K_k}	Whole cell conductance of K^+	6907.77 μM mV^{-1} s^{-1}
G_{Na_k}	Whole cell conductance of Na^+	226.94 μM mV^{-1} s^{-1}
G_{NBC_k}	Whole cell conductance of the NBC cotransporter	130.74 μM mV^{-1} s^{-1}
G_{KCC1_k}	Whole cell conductance of the KCC1 cotransporter	1.728 μM mV^{-1} s^{-1}
G_{NKCC1_k}	Whole cell conductance of the NKCC1 cotransporter	9.568 μM mV^{-1} s^{-1}
G_{BK_k}	Whole cell conductance of the BK channel	10.25 μM mV^{-1} s^{-1}
G_{Cl_k}	Whole cell conductance of Cl^-	151.93 μM mV^{-1} s^{-1}
G_{TRPV_k}	Whole cell conductance of TRPV4 channel	3.15e-4 μM mV^{-1} s^{-1}
$J_{NaK_{max}}$	Maximum flux through the Na^+/K^+ ATP-ase pump	2.37×10^4 μM s^{-1}
K_{Na_k}	Na^+/K^+ ATP-ase pump constant	10×10^3 μM
K_{K_s}	Na^+/K^+ ATP-ase pump constant	1.5×10^3 μM
ρ_{min}	Minimum ratio of bound to unbound IP_3 receptors	0.1
ρ_{max}	Maximum ratio of bound to unbound IP_3 receptors	0.7
δ_G	Ratio of the activities of the unbound and bound receptors	1.235×10^{-2}
K_G	G-protein disassociation constant	8.82
r_h	Maximum rate of IP_3 production in astrocyte due to glutamate receptors	4.8 μM s^{-1}
k_{deg}	Rate constant for IP_3 degradation in astrocyte	1.25 s^{-1}
r_{buff}	Rate of Ca^{2+} buffering at the endfoot compared to the astrocyte body	0.05
VR_{ERcyt}	Volume ratio between ER and astrocytic cytosol	0.185
BK_{end}	Ratio of endogenous buffer concentration to disassociation constant	40
K_{ex}	Disassociation constant of exogenous buffer	0.26 μM
B_{ex}	Concentration of exogenous buffer	11.35 μM
J_{max}	Maximum rate of Ca^{2+} through the IP_3 mediated channel	2880 μM s^{-1}
K_i	Disassociation constant for IP_3 binding to an IP_3R	0.03 μM

K_{act_k}	Disassociation constant for Ca^{2+} binding to an activation site on an IP_3R	0.17 μM
k_{on}	Rate of Ca^{2+} binding to the inhibitory site on the IP_3R	2 μM $^{-1}$ s^{-1}
K_{inh}	Disassociation constant of IP_3R	0.1 μM
V_{max}	Maximum rate of Ca^{2+} uptake pump on the ER	20 μM s^{-1}
k_{pump}	Ca^{2+} uptake pump disassociation constant	0.24 μM
P_L	ER leak channel steady state balance constant	0.0804 μM s^{-1}
V_{eet}	EET production rate	72 s^{-1}
$c_{k_{min}}$	Minimum Ca^{2+} concentration required for EET production	0.1 μM
k_{eet}	EET degradation rate	7.2 s^{-1}
v_4	Measure of the spread of w_∞	8 mV
eet_{shift}	Describes the EET dependent voltage shift	2 mV μM $^{-1}$
v_5	Determines the range of the shift of w_∞ as Ca^{2+} varies	15 mV
v_6	Shifts the range of w_∞	-55 mV
ψ_n	Characteristic time for the opening of the BK channel	2.664 s^{-1}
Ca_3	BK open probability Ca^{2+} constant	0.4 μM
Ca_4	BK open probability Ca^{2+} constant	0.35 μM
AA_m	dissociation constant for AA_k	0.161 μM
AA_{max}	maximum rate of generation of AA_k	29 μM s^{-1}
Ca_0	baseline Ca_k^{2+}	0.1432 μM
D_{AA}	diffusion coefficient for AA	0.152 $\mu m^2 ms^{-1}$
E_{GABA}	Nernst potential for GABA	-75 mV
g_{mid}	midpoint of the GABA sigmoidal	0.6
g_{slope}	scaling for the GABA sigmoidal	0.1
C_k	V_{max} for astrocyte CICR	30 μM ms^{-1}
sc_k	first Disassociation constant for astrocytic CICR flux	2 μM
cc_k	second Disassociation constant for astrocytic CICR flux	0.9 μM

Table 7: Parameters of the astrocyte and SC submodel, for references see Dormanns et al. [5], Kenny et al. [10].

8 PVS

8.1 ODEs

K^+ concentration in the PVS (μM):

$$\frac{dK_p}{dt} = \frac{J_{BK_k}}{VR_{pk}} + \frac{J_{KIR_i}}{VR_{pi}} - K_{decay_p}(K_p - K_{min_p}) \tag{111}$$

Ca^{2+} concentration in the PVS (μM):

$$\frac{dCa_p}{dt} = \frac{J_{TRPV_k}}{VR_{pk}} + \frac{J_{VOCC_i}}{VR_{pi}} - Ca_{decay_p}(Ca_p - Ca_{min_p}) \tag{112}$$

The open probability of the transient receptor potential vanniloid-related 4 (TRPV4) channel (-):

$$\frac{dm_k}{dt} = \frac{m_{\infty_k} - m_k}{t_{TRPV_k}} \tag{113}$$

8.2 Algebraic Variables

The flux of Ca^{2+} through the VOCC which connects the SMC to the PVS (μM s^{-1}):

$$J_{VOCC_i} = G_{Cai} \frac{v_i - v_{Ca1}}{1 + \exp\left[-(v_i - v_{Ca2})/R_{Cai}\right]} \tag{114}$$

This VOCC channel is altered when the interneuron model is used. See below equation (150)

The flux of Ca^{2+} through the TRPV4 channel (μM s^{-1}):

$$J_{TRPV_k} = G_{TRPV_k} m_k (v_k - E_{TRPV_k}) \tag{115}$$

The Nernst potential of the TRPV4 channel (mV):

$$E_{TRPV_k} = \frac{\phi}{z_{Ca}} \ln\left(\frac{Ca_p}{Ca_k}\right) \tag{116}$$

The equilibrium state of the TRPV4 channel (-):

$$m_{\infty_k} = \Gamma_m \left[\frac{1}{1 + H_{Ca_k}} \left(H_{Ca_k} + \tanh\left(\frac{v_k - v_{1,TRPV}}{v_{2,TRPV}}\right)\right)\right] \tag{117}$$

The material strain gating term (-):

$$\Gamma_m = \frac{1}{1 + \exp\left(-\frac{\eta - \eta_0}{\kappa_k}\right)} \tag{118}$$

The strain on the perivascular endfoot of the astrocyte (-)

$$\eta = \frac{R - R_{init}}{R_{init}} \tag{119}$$

The Ca^{2+} inhibitory term (-)

$$H_{Ca_k} = \frac{Ca_k}{\gamma_{Cai}} + \frac{Ca_p}{\gamma_{Cae}} \tag{120}$$

Parameter	Description	Value
VR_{pk}	Volume ratio between PVS and astrocyte	0.001
VR_{pi}	Volume ratio between PVS and SMC	0.001
K_{decay_p}	Rate of decay of K^+ in PVS	0.15 s^{-1}
K_{min_p}	Steady state value of K^+ in PVS	3×10^3 μM
Ca_{decay_p}	Rate of decay of Ca^{2+} in PVS	0.5 s^{-1}
Ca_{min_p}	Steady state value of Ca^{2+} in PVS	2×10^3 μM
G_{Cai}	VOCC whole cell conductance	1.29×10^{-3} μM mV^{-1} s^{-1}
v_{Ca1}	VOCC reversal potential	100 mV
v_{Ca2}	Half point of the VOCC activation sigmoidal	-24 mV
R_{Cai}	Maximum slope of the VOCC activation sigmoidal	8.5 mV
G_{TRPV_k}	TRPV4 whole cell conductance	3.15×10^{-4} μM mV^{-1} s^{-1}
t_{TRPV_k}	Characteristic time constant for m_k	0.9 s
η_0	Strain required for half activation of the TRPV4 channel	0.1
κ_k	TRPV4 channel strain constant	0.1
$v_{1,TRPV}$	TRPV4 channel voltage gating constant	120 mV
$v_{2,TRPV}$	TRPV4 channel voltage gating constant	13 mV
γ_{Cai}	Ca^{2+} concentration constant	0.01 μM
γ_{Cae}	Ca^{2+} concentration constant	200 μM

Table 8: Parameters of the PVS compartment, for references see Dormanns et al. [5], Kenny et al. [10].

9 SMC

9.1 ODEs

Cytosolic Ca^{2+} in the SMC (μM):

$$\begin{aligned}\frac{dCa_i}{dt} = J_{IP_{3i}} - J_{SR_{uptake_i}} + J_{CICR_i} - J_{extrusion_i} + J_{SR_{leak_i}} \dots \\ -J_{VOCC_i} + J_{Na/Ca_i} - 0.1J_{stretch_i} + J^{SMC-EC}_{Ca^{2+}-coupling_i}\end{aligned} \tag{121}$$

Ca^{2+} in the sarcoplasmic reticulum (SR) of the SMC (μM):

$$\frac{ds_i}{dt} = J_{SR_{uptake_i}} - J_{CICR_i} - J_{SR_{leak_i}} \tag{122}$$

Membrane potential of the SMC (mV):

$$\frac{dv_i}{dt} = -\gamma_v(J_{NaK_i} + J_{Cl_i} + 2J_{VOCC_i} + J_{Na/Ca_i} + J_{K_i} + J_{stretch_i} + J_{KIR_i}) + V^{SMC-EC}_{coupling_i} \tag{123}$$

Open state probability of Ca^{2+}-activated K^+ channels (-):

$$\frac{dw_i}{dt} = \lambda_i \left(K_{act_i} - w_i\right) \tag{124}$$

IP_3 concentration in the SMC (μM):

$$\frac{dIP3_i}{dt} = -J_{degrad_i} + J^{SMC-EC}_{IP_3-coupling_i} \tag{125}$$

Arachidonic acid in the SMC, this is just diffused from the astrocyte.

$$\tau_{AA} = \frac{x^2_{ki}}{D_{AA}} \tag{126}$$

$$\frac{dAA_i}{dt} = \frac{AA_k - AA_i}{\tau_{AA}} \tag{127}$$

20-HETE in the SMC

$$\frac{dH_i}{dt} = \frac{1}{1 + exp(\frac{(NO_i - NO_{rest})}{R_{NO}})} \frac{V_a AA_i}{K_a + AA_i} + \frac{V_f AA_i}{K_f + AA_i} - \lambda_h H_i \tag{128}$$

$$\tag{129}$$

Here there are two CYP generators of 20-HETE . The CYP450 generator is inhibited by NO hence the function multiplying the first term of the o.d.e. for 20-HETE. This model is a phenomenological one and relies on the results from [13]

9.2 Algebraic Variables

Release of Ca^{2+} from IP_3 sensitive stores in the SMC (μM s^{-1}):

$$J_{IP3_i} = F_i \frac{IP3_i^2}{K_{ri}^2 + IP3_i^2} \tag{130}$$

Uptake of Ca^{2+} into the SR (μM s^{-1}):

$$J_{SR_{uptake_i}} = B_i \frac{Ca_i^2}{c_{bi}^2 + Ca_i^2} \tag{131}$$

Ca^{2+} induced Ca^{2+} release (CICR) (μM s^{-1}):

$$J_{CICR_i} = C_i \frac{s_i^2}{s_{ci}^2 + s_i^2} \frac{Ca_i^4}{c_{ci}^4 + Ca_i^4} \tag{132}$$

Ca^{2+} extrusion by Ca^{2+}-ATP-ase pumps (μM s^{-1}):

$$J_{extrusion_i} = D_i Ca_i \left(1 + \frac{v_i - v_d}{R_{di}}\right) \tag{133}$$

Leak current from the SR (μM s^{-1}):

$$J_{SR_{leak_i}} = L_i s_i \tag{134}$$

Flux of Ca^{2+} exchanging with Na^+ in the Na^+/Ca^{2+} exchange (μM s^{-1}):

$$J_{Na/Ca_i} = G_{Na/Ca_i} \frac{Ca_i}{Ca_i + c_{Na/Cai}} \left(v_i - v_{Na/Ca_i}\right) \tag{135}$$

Ca^{2+} flux through the stretch-activated channels in the SMC (μM s^{-1}):

$$J_{stretch_i} = \frac{G_{stretch}}{1 + \exp\left(-\alpha_{stretch}\left(\frac{\Delta pR}{h} - \sigma_0\right)\right)} \left(v_i - E_{SAC}\right) \tag{136}$$

Flux through the Na^+/K^+ pump (μM s^{-1}):

$$J_{NaK_i} = F_{NaK} \tag{137}$$

Cl^- flux through the Cl^- channel (μM s^{-1}):

$$J_{Cl_i} = G_{Cli}\left(v_i - v_{Cli}\right) \tag{138}$$

K^+ flux through K^+ channel (μM s^{-1}):

$$J_{K_i} = G_{Ki} w_i \left(v_i - v_{K_i}\right) \tag{139}$$

Flux through inward rectifying K^+ (KIR) channels in the SMC (μM s^{-1}):

$$J_{KIR_i} = G_{KIR_i}(v_i - v_{KIR_i}) \tag{140}$$

IP_3 degradation (μM s^{-1}):

$$J_{degrad_i} = k_{di} IP3_i \tag{141}$$

Nernst potential of the KIR channel in the SMC (mV):

$$v_{KIR_i} = z_1 K_p - z_2 \tag{142}$$

Conductance of KIR channel (μM mV^{-1} s^{-1}):

$$G_{KIR_i} = F_{KIR_i} \exp(z_5 v_i + z_3 K_p - z_4) \tag{143}$$

Equilibrium distribution of open channel states for the SMC BK channels (-):

$$K_{act_i} = \frac{\left(Ca_i + c_{w,i}\right)^2}{\left(Ca_i + c_{w,i}\right)^2 + \alpha_{act_i} \exp(-\left([v_i - v_{Ca3i} - h_{shift}(H_i - H_0)\right]/R_{Ki}))} \tag{144}$$

Translation factor, regulatory effect of cyclic guanosine monophosphate (cGMP) on the BK channel open probability (μM):

$$c_{\mathrm{w},i} = \frac{\beta_{w,i}}{2}(1 + \tanh\left(\frac{\mathrm{cGMP}_i - \alpha_{w,i}}{\epsilon_{w,i}}\right)) \tag{145}$$

Heterocellular electrical coupling between SMCs and ECs (mV s^{-1}):

$$V_{coupling_i}^{SMC-EC} = -G_{coup}(v_i - v_j) \tag{146}$$

Heterocellular IP_3 coupling between SMCs and ECs (μM s^{-1}):

$$J_{IP_3-coupling_i}^{SMC-EC} = -P_{IP_3}(IP3_i - IP3_j) \tag{147}$$

Ca^{2+} coupling between SMCs and ECs (μM s^{-1}):

$$J_{Ca^{2+}-coupling_i}^{SMC-EC} = -P_{Ca^{2+}}(Ca_i - Ca_j) \tag{148}$$

Finally the flux of Ca^{2+} through the VOCC channel on the SMC is given by

$$J_{VOCC,i} = g_{VOCC}\frac{v_i - v_{Ca1}}{1 + \exp\left(\frac{-(v_i - v_{Ca2})}{R_{Ca}}\right)} \tag{149}$$

which is the same as equation (114) where $v_{Ca1} = 100$ mV is the reversal potential, $v_{Ca2} = -24$ mV is the half-point of the VOCC activation sigmoidal, and $R_{Ca} = 8.5$ mV is the maximum slope of the sigmoidal (all taken from the NVU model). However for the interneuron model the NPY conductance is given by

$$g_{VOCC} = G_{Ca,i}\left(1 + \frac{N_{inc}}{2}\tanh\left(\frac{NPY_N - N_{mid}}{N_{slope}}\right)\right) \tag{150}$$

where $G_{Ca,i} = 1.29 \times 10^{-6}$ μM mV^{-1} ms^{-1} is the base conductance of the VOCC (taken from the NVU model), $N_{inc} = 0.05$ is the proportional increase of the conductance from baseline due to NPY (i.e. 0.05 means a 5% increase from $G_{Ca,i}$ when NPY is released, model estimate), $N_{mid} = 0.6$ is the midpoint of the sigmoidal, and N_{slope} is the slope of the sigmoidal (both model estimates). Hence when $NPY_N = 0$, $g_{VOCC} = G_{Ca,i}$ and when $NPY_N = 1$, $g_{VOCC} = 1.05 \times G_{Ca,i}$.

Parameter	Description	Value
λ_i	Rate constant for opening	45 s^{-1}
F_i	Maximal rate of activation-dependent Ca^{2+} influx	0.23 μM s^{-1}
K_{ri}	Half-saturation constant for agonist-dependent Ca^{2+} entry	1 μM
B_i	SR uptake rate constant	2.025 μM s^{-1}
c_{bi}	Half-point of the SR ATP-ase activation sigmoidal	1 μM
C_i	CICR rate constant	55 μM s^{-1}
s_{ci}	Half-point of the CICR Ca^{2+} efflux sigmoidal	2 μM
c_{ci}	Half-point of the CICR activation sigmoidal	0.9 μM
D_i	Rate constant for Ca^{2+} extrusion by the ATP-ase pump	0.24 s^{-1}
v_d	Intercept of voltage dependence of extrusion ATP-ase	-100 mV
R_{di}	Slope of voltage dependence of extrusion ATP-ase	250 mV
L_i	Leak from SR rate constant	0.025 s^{-1}
G_{Cai}	Whole-cell conductance for VOCCs	1.29×10^{-3} μM mV^{-1} s^{-1}
$v_{Ca_{1i}}$	Reversal potential for VOCCs	100 mV
$v_{Ca_{2i}}$	Half-point of the VOCC activation sigmoidal	-24 mV
R_{Cai}	Maximum slope of the VOCC activation sigmoidal	8.5 mV
$G_{Na/Cai}$	Whole-cell conductance for Na^+/Ca^{2+} exchange	3.16×10^{-3} μM mV^{-1} s^{-1}
$c_{Na/Cai}$	Half-point for activation of Na^+/Ca^{2+} exchange by Ca^{2+}	0.5 μM
$v_{Na/Cai}$	Reversal potential for the Na^+/Ca^{2+} exchanger	-30 mV
$G_{stretch}$	Whole cell conductance for stretch activated channels (SACs)	6.1×10^{-3} μM mV^{-1} s^{-1}

$\alpha_{stretch}$	Slope of stress dependence of the SAC activation sigmoidal	7.4×10^{-3} mmHg^{-1}
Δp	Pressure difference over vessel	30 mmHg
σ_0	Half-point of the SAC activation sigmoidal	500 mmHg
E_{SAC}	Reversal potential for SACs	-18 mV
F_{NaK}	Rate of the K^+ influx by the Na^+/K^+ pump	4.32×10^{-2} μM s^{-1}
G_{Cli}	Whole-cell conductance for Cl^- current	1.34×10^{-3} μM mV^{-1} s^{-1}
v_{Cli}	Reversal potential for Cl^- channels	-25 mV
G_{Ki}	Whole-cell conductance for K^+ efflux	4.46×10^{-3} μM mV^{-1} s^{-1}
v_{K_i}	Nernst potential	-94 mV
k_{di}	Rate constant of IP_3 degradation	0.1 s^{-1}
F_{KIR_i}	Scaling factor of K^+ efflux through the KIR channel	$1.285\times10^{-6}\mu$M mV^{-1} s^{-1}
z_1	Model estimation for membrane voltage KIR channel	4.5×10^3 mV μM $^{-1}$
z_2	Model estimation for membrane voltage KIR channel	112 mV
z_3	Model estimation for the KIR channel conductance	4.2×10^{-4} μM $^{-1}$
z_4	Model estimation for the KIR channel conductance	12.6
z_5	Model estimation for the KIR channel conductance	-7.4×10^{-2} mV^{-1}
α_{act_i}	Translation factor for v_i dependence of K_{act_i} sigmoidal	0.13 μM ^{2}
$v_{Ca_{3i}}$	Half-point for the K_{act_i} activation sigmoidal	-27 mV
R_{Ki}	Maximum slope of the K_{act_i} activation sigmoidal	12 mV
h_{shift}	20-HETE scaling parameter in K_{act_i} activation sigmoidal	10
H_0	20-HETE shift parameter in K_{act_i} activation sigmoidal	0.126 μM
λ_h	20-HETE degradation parameter	2.0e-3 s^{-1}
$\beta_{w,i}$	Constant to fit data	1 μM
$\alpha_{w,i}$	Constant to fit data	10.75 μM
$\epsilon_{w,i}$	Constant to fit data	0.668 μM
G_{coup}	Heterocellular electrical coupling coefficient	0.5 s^{-1}
P_{IP_3}	Heterocellular IP_3 coupling coefficient	0.05 s^{-1}
$P_{Ca^{2+}}$	Heterocellular $P_{Ca^{2+}}$ coupling coefficient	0.05 s^{-1}

Table 9: Parameters of the SMC compartment, for references see Dormanns et al. [5].

10 EC

10.1 ODEs

Cytosolic Ca^{2+} concentration in the EC (μM):

$$\begin{aligned}\frac{dCa_j}{dt} = J_{IP_{3j}} - J_{ER_{uptake_j}} + J_{CICR_j} - J_{extrusion_j} \cdots \\ + J_{ER_{leak_j}} + J_{cation_j} + J_{0_j} - J_{stretch_j} - J^{SMC-EC}_{Ca^{2+}-coupling_j}\end{aligned} \tag{151}$$

Ca^{2+} concentration in the ER in the EC (μM):

$$\frac{ds_j}{dt} = J_{ER_{uptake_j}} - J_{CICR_j} - J_{ER_{leak_j}} \tag{152}$$

Membrane potential of the EC (mV):

$$\frac{dv_j}{dt} = -\frac{1}{C_{m_j}}(I_{K_j} + I_{R_j}) - V^{SMC-EC}_{coupling_j} \tag{153}$$

IP_3 concentration of the EC (μM):

$$\frac{dIP3_j}{dt} = J_{PLC} - J_{degrad_j} - J^{SMC-EC}_{IP_3-coupling_j} \tag{154}$$

10.2 Algebraic Variables

Release of Ca^{2+} from IP_3-sensitive stores in the EC (μM s^{-1}):

$$J_{IP_{3j}} = F_j \frac{IP3_j^2}{K_{rj}^2 + IP3_j^2} \tag{155}$$

Uptake of Ca^{2+} into the endoplasmic reticulum (μM s^{-1}):

$$J_{ER_{uptake_j}} = B_j \frac{Ca_j^2}{c_{bj}^2 + Ca_j^2} \tag{156}$$

CICR (μM s^{-1}):

$$J_{CICR_j} = C_j \frac{s_j^2}{s_{cj}^2 + s_j^2} \frac{Ca_j^4}{c_{cj}^4 + Ca_j^4} \tag{157}$$

Ca^{2+} extrusion by Ca^{2+}-ATP-ase pumps (μM s^{-1}):

$$J_{extrusion_j} = D_j Ca_j \tag{158}$$

Ca^{2+} flux through the stretch-activated channels in the EC (μM s^{-1}):

$$J_{stretch_j} = \frac{G_{stretch}}{1 + \exp\left(-\alpha_{stretch}\left(\frac{\Delta pR}{h} - \sigma_0\right)\right)} (v_j - E_{SAC}) \tag{159}$$

Leak current from the ER (μM s^{-1}):

$$J_{ER_{leak_j}} = L_j s_j \tag{160}$$

Ca^{2+} influx through nonselective cation channels (μM s^{-1}):

$$J_{cation_j} = G_{cat_j}(E_{Ca_j} - v_j)\frac{1}{2}\left(1 + \tanh\left(\frac{\log_{10}(Ca_j/c_{log}) - m_{3_{cat_j}}}{m_{4_{cat_j}}}\right)\right) \tag{161}$$

K^+ current through the BK_{Caj} channel and the SK_{Caj} channel (fA):

$$I_{K_j} = G_{totj}(v_j - v_{Kj})\left(I_{BK_{Caj}} + I_{SK_{Caj}}\right) \tag{162}$$

K^+ efflux through the BK_{Caj} channel (-):

$$I_{BK_{Caj}} = 0.2\left(1 + \tanh\left(\frac{(\log_{10}(Ca_j/c_{log}) - c)(v_j - b_j) - a_{1j}}{m_{3bj}(v_j + a_{2j}(\log_{10}(Ca_j/c_{log}) - c) - b_j)^2 + m_{4bj}}\right)\right) \tag{163}$$

K^+ efflux through the SK_{Caj} channel (-):

$$I_{SK_{Caj}} = 0.3\left(1 + \tanh\left(\frac{\log_{10}(Ca_j/c_{log}) - m_{3sj}}{m_{4sj}}\right)\right) \tag{164}$$

Residual current regrouping Cl^- and Na^+ current flux (fA):

$$I_{R_j} = G_{R_j}(v_j - v_{restj}) \tag{165}$$

IP_3 degradation (μM s^{-1}):

$$J_{degrad_j} = k_{dj} IP3_j \tag{166}$$

coupling between SMC and EC

membrane coupling

$$V_{coupling_j}^{SMC-EC} = G_{coup}(v_i - v_j) \tag{167}$$

Ca^{2+} coupling

$$J_{Ca^{2+}-coupling_j}^{SMC-EC} = Ca_{coup}(Ca_i - Ca_j) \tag{168}$$

IP_3 coupling

$$J_{IP_3-coupling_j}^{SMC-EC} = IP_{3,coup}(I_i - I_j) \tag{169}$$

Parameter	Description	Value
J_{0_j}	Constant Ca^{2+} influx	0.029 μM s^{-1}
C_{m_j}	Membrane capacitance	25.8 pF
J_{PLC}	IP_3 production rate	0.11 μM s^{-1}
F_j	Maximal rate of activation-dependent Ca^{2+} influx	0.23 μM s^{-1}
K_{rj}	Half-saturation constant for agonist-dependent Ca^{2+} entry	1 μM
B_j	ER uptake rate constant	0.5 μM s^{-1}
c_{bj}	Half-point of the SR ATP-ase activation sigmoidal	1 μM
C_j	CICR rate constant	5 μM s^{-1}
s_{cj}	Half-point of the CICR Ca^{2+} efflux sigmoidal	2 μM
c_{cj}	Half-point of the CICR activation sigmoidal	0.9 μM
D_j	Rate constant for Ca^{2+} extrusion by the ATP-ase pump	0.24 s^{-1}
L_j	Rate constant for Ca^{2+} leak from the ER	0.025 s^{-1}
G_{catj}	Whole-cell cation channel conductivity	6.6×10^{-4} μM mV^{-1} s^{-1}
E_{Caj}	Ca^{2+} equilibrium potential	50 mV
c_{log}	Log constant	1 μM
G_{totj}	Total K^+ channel conductivity	6927 pS
v_{Kj}	K^+ equilibrium potential	-80 mV
$m_{3_{catj}}$	Model constant, further explanation see [11]	-0.18
$m_{4_{catj}}$	Model constant, further explanation see [11]	0.37
c	Model constant, further explanation see [11]	-0.4
b_j	Model constant, further explanation see [11]	-80.8 mV
a_{1j}	Model constant, further explanation see [11]	53.3 mV
a_{2j}	Model constant, further explanation see [11]	53.3 mV
m_{3bj}	Model constant, further explanation see [11]	1.32×10^{-3} mV^{-1}
m_{4bj}	Model constant, further explanation see [11]	0.30 mV
m_{3sj}	Model constant, further explanation see [11]	-0.28
m_{4sj}	Model constant, further explanation see [11]	0.389
G_{R_j}	Residual current conductivity	955 pS
v_{restj}	Membrane resting potential	-31.1 mV
k_{dj}	Rate constant of IP_3 degradation	0.1 s^{-1}
G_{coup}	coupling coefficient for membrane potential	0.5 s^{-1}
Ca_{coup}	coupling coefficient for Ca^{2+}	0.05 s^{-1}
$IP_{3,coup}$	coupling coefficient for IP_3	0.05 s^{-1}

Table 10: Parameters of the EC compartment, for references see Dormanns et al. [5].

11 NO pathway

11.1 ODEs

Ca^{2+} concentration in the neuron (μM):

$$\frac{dCa_n}{dt} = \frac{1}{1+\lambda_{\text{buf}}}\left(\frac{I_{\text{Ca,tot}}}{2FV_{\text{spine}}} - \kappa_{\text{ex}}(Ca_n - [Ca]_{\text{rest}})\right) \tag{170}$$

Activated nNOS (μM):

$$\frac{d[\text{nNOS}]_n}{dt} = \frac{V_{\text{max,nNOS}}[\text{CaM}]_n}{K_{\text{m,nNOS}} + [\text{CaM}]_n} - \mu_{\text{deact},n}[\text{nNOS}]_n \tag{171}$$

we have changed some of the parameters for this nNOS equation to get a more reasonable profile see Table 11. These values give a maximum $nNOS_{act}$ of 0.2408 μM. Because of this change initial values for all state variables have been changed (only slightly) to reflect the new vaues of $nNOS_{act}$ and NO.

NO concentration in the neuron (μM):

$$\frac{d\text{NO}_n}{dt} = p_{NO,n} - c_{NO,n} + d_{NO,n} \tag{172}$$

NO concentration in the astrocyte (μM):

$$\frac{d\text{NO}_k}{dt} = p_{NO,k} - c_{NO,k} + d_{NO,k} \tag{173}$$

NO concentration in the SMC (μM):

$$\frac{d\text{NO}_i}{dt} = p_{NO,i} - c_{NO,i} + d_{NO,i} \tag{174}$$

Activated endothelial NO synthase (eNOS) (μM):

$$\frac{d[\text{eNOS}]_j}{dt} = \gamma_{\text{eNOS}}\frac{K_{\text{dis}}Ca_j}{K_{\text{m,eNOS}} + Ca_j} + (1-\gamma_{\text{eNOS}})g_{\max}F_{\text{wss}} - \mu_{\text{deact},j}[\text{eNOS}]_j \tag{175}$$

NO concentration in the EC (μM):

$$\frac{d\text{NO}_j}{dt} = p_{NO,j} - c_{NO,j} + d_{NO,j} \tag{176}$$

Fraction of soluble guanylyl cyclase (sGC) in the basal state (-):

$$\frac{dE_b}{dt} = -k_1 E_b \text{NO}_i + k_{-1}E_{6c} + k_4 E_{5c} \tag{177}$$

Fraction of sGC in the intermediate form (-):

$$\frac{dE_{6c}}{dt} = k_1 E_b \text{NO}_i - (k_{-1}+k_2)E_{6c} - k_3 E_{6c}\text{NO}_i \tag{178}$$

Concentration of cGMP in the SMC (μM):

$$\frac{d\text{cGMP}_i}{dt} = V_{\text{max,sGC}}E_{5c} - V_{\text{max,pde}}\frac{\text{cGMP}_i}{K_{\text{m,pde}} + \text{cGMP}_i} \tag{179}$$

11.2 Algebraic Variables

Fraction of open NR2A N-methyl-D-aspartate (NMDA) receptors (-):

$$w_{\text{NR2},A} = \frac{Glu}{K_{m,A} + Glu} \tag{180}$$

Fraction of open NR2B NMDA receptors (-):

$$w_{\text{NR2},B} = \frac{Glu}{K_{\text{m},B} + Glu} \tag{181}$$

Inward Ca^{2+} current per open NMDA receptor (fA):

$$I_{\text{Ca}} = \frac{4v_n G_{\text{M}}(P_{\text{Ca}}/P_{\text{M}})([Ca]_{\text{ex}}/[\text{M}])}{1+\exp(\alpha_v(v_n+\beta_v))} \frac{\exp(2v_n/\phi))}{1-\exp(2v_n/\phi))} \tag{182}$$

Total inward Ca^{2+} current for all open NMDA receptors per synapse (fA):

$$I_{\text{Ca,tot}} = (n_{\text{NR2},A} w_{\text{NR2},A} + n_{\text{NR2},B} w_{\text{NR2},B}) I_{\text{Ca}} \tag{183}$$

Ca^{2+}-calmodulin complex concentration (μM):

do we use Ca^{2+}-calmodulin complex at all?

$$[\text{CaM}]_n = \frac{Ca_n}{m_c} \tag{184}$$

Neuronal NO production flux (μM s^{-1}):

$$p_{NO,n} = V_{\text{max,NO},n}[\text{nNOS}]_n \frac{[O_2]_n}{K_{\text{m,O2},n} + [O_2]_n} \frac{[LArg]_n}{K_{\text{m,LArg},n} + [LArg]_n} \tag{185}$$

Neuronal NO consumption flux (μM s^{-1}):

$$c_{NO,n} = k_{\text{O2},n}[\text{NO}]_n^2 [O_2]_n \tag{186}$$

Neuronal NO diffusive flux (μM s^{-1}):

$$d_{NO,n} = \frac{[\text{NO}]_k - [\text{NO}]_n}{\tau_{nk}} \tag{187}$$

Time for NO to diffuse between the centres of the neuron and the astrocyte (s):

$$\tau_{nk} = \frac{x_{nk}^2}{2D_{\text{c,NO}}} \tag{188}$$

Astrocytic NO production flux (μM s^{-1}):

$$p_{NO,k} = 0 \tag{189}$$

Astrocytic NO consumption flux (μM s^{-1}):

$$c_{NO,k} = k_{\text{O2},k}[\text{NO}]_k^2 [O_2]_k \tag{190}$$

Astrocytic NO diffusive flux (μM s^{-1}):

$$d_{NO,k} = \frac{[\text{NO}]_n - [\text{NO}]_k}{\tau_{nk}} + \frac{[\text{NO}]_i - [\text{NO}]_k}{\tau_{ki}} \tag{191}$$

Time for NO to diffuse between the centres of the astrocyte and the SMC (s):

$$\tau_{ki} = \frac{x_{ki}^2}{2D_{\text{c,NO}}} \tag{192}$$

SMC NO production flux (μM s^{-1}):

$$p_{NO,i} = 0 \tag{193}$$

SMC NO consumption flux (μM s^{-1}):

$$c_{NO,i} = k_{\text{dno}}[\text{NO}]_i \tag{194}$$

SMC NO diffusive flux (μM s^{-1}):

$$d_{NO,i} = \frac{[\text{NO}]_k - [\text{NO}]_i}{\tau_{ki}} + \frac{[\text{NO}]_j - [\text{NO}]_i}{\tau_{ij}} \tag{195}$$

sGC kinetics rate constant (s^{-1}):

$$k_4 = C_4[\text{cGMP}]_i^2 \tag{196}$$

Fraction of sGC in the fully activated form (-):

$$E_{5c} = 1 - E_b - E_{6c} \tag{197}$$

Regulatory effect of cGMP on myosin dephosphorylation (-):

$$R_{\text{cGMP}} = \frac{[\text{cGMP}]_i^2}{K_{\text{m,mlcp}}^2 + [\text{cGMP}]_i^2} \tag{198}$$

Maximum cGMP production rate (μM s^{-1}):

$$V_{\text{max,pde}} = k_{\text{pde}}[\text{cGMP}]_i \tag{199}$$

Time for NO to diffuse between the centres of the SMC and the EC (s):

$$\tau_{ij} = \frac{x_{ij}^2}{2D_{\text{c,NO}}} \tag{200}$$

Fraction of the elastic strain energy stored within the membrane (-):

$$F_{\text{wss}} = \frac{1}{1 + \alpha_{\text{wss}} \exp(-W_{\text{wss}})} - \frac{1}{1 + \alpha_{\text{wss}}} \tag{201}$$

Strain energy density (-):

$$W_{\text{wss}} = W_0 \frac{(\tau_{\text{wss}} + \sqrt{16\delta_{\text{wss}}^2 + \tau_{\text{wss}}^2} - 4\delta_{\text{wss}})^2}{\tau_{\text{wss}} + \sqrt{16\delta_{\text{wss}}^2 + \tau_{\text{wss}}^2}} \tag{202}$$

Wall shear stress (Pa):

$$\tau_{\text{wss}} = \frac{R\Delta P}{2L} \tag{203}$$

O_2 concentration in the EC (μM):

$$[O_2]_j = c_{unit}\, O_2 \tag{204}$$

Oxygen in EC taken as O_2 from lumen (diffusion very fast so plausible!) instead of constant, in uM, hence $c_{unit} = 1$.
EC NO production flux (μM s^{-1}):

$$p_{NO,j} = V_{\text{max,NO},j}[\text{eNOS}]_j \frac{[O_2]_j}{K_{\text{m,O2},j} + [O_2]_j} \frac{[LArg]_j}{K_{\text{m,L-Arg},j} + [LArg]_j} \tag{205}$$

EC NO consumption flux (μM s^{-1}):

$$c_{NO,j} = k_{\text{O2},j}[\text{NO}]_j^2[O_2]_j \tag{206}$$

EC NO diffusive flux (μM s^{-1}):

$$d_{NO,j} = \frac{[\text{NO}]_i - [\text{NO}]_j}{\tau_{ij}} - \frac{4D_{\text{c,NO}}[\text{NO}]_j}{r_l^2} \tag{207}$$

Parameter	Description	Value
$[\text{Glu}]_{\max}$	Maximum glutamate concentration	1846 μM
λ_{buf}	Buffer capacity	20
V_{spine}	Dendritic spine volume	8×10^{-5} pL
κ_{ex}	Decay rate constant of internal Ca^{2+} concentration	1.6×10^{3} s^{-1}
$[Ca]_{\text{rest}}$	Resting internal Ca^{2+} concentration	0.1 μM
$V_{\text{max,nNOS}}$	Maximum nNOS activation rate	0.7×10^{-3} μM s^{-1} new values
$K_{\text{m,nNOS}}$	Michaelis constant	0.8 μM new values
$\mu_{\text{deact},n}$	Rate constant at which nNOS is deactivated	0.02 s^{-1} new values
$K_{\text{m},A}$	Michaelis constant	650 μM
$K_{\text{m},B}$	Michaelis constant	2800 μM
v_n	Neuronal membrane potential	-40 mV
G_{M}	Conductance of NMDA receptor	0.46 pS new value
$P_{\text{Ca}}/P_{\text{M}}$	Ratio of Ca^{2+} permeability to monovalent ion permeability	3.6
$[Ca]_{\text{ex}}$	External Ca^{2+} concentration	2×10^{3} μM
[M]	Concentration of monovalent ions	1.3×10^{5} μM
α_v	Voltage-dependent Mg^{2+} block parameter	-0.08 mV^{-1}
β_v	Voltage-dependent Mg^{2+} block parameter	20 mV
$n_{\text{NR2},A}$	Average number of NR2A NMDA receptors	0.63
$n_{\text{NR2},B}$	Average number of NR2B NMDA receptors	11
m_c	Number of Ca^{2+} ions bound per calmodulin	4
$V_{\text{max,NO},n}$	Maximum catalytic rate of neuronal NO production	4.22 s^{-1}
$[O_2]_n$	O_2 concentration in the neuron	200 μM
$K_{\text{m,O2},n}$	Michaelis constant for nNOS for O_2	243 μM
$[LArg]_n$	L-Arg concentration in the neuron	100 μM
$K_{\text{m,LArg},n}$	Michaelis constant for nNOS for LArg	1.5 μM
$k_{\text{O2},n}$	O_2 reaction rate constant	9.6×10^{-6} μM $^{-2}$ s^{-1}
x_{nk}	Distance between centres of neuron and astrocyte	25 μm
$k_{\text{O2},k}$	O_2 reaction rate constant	$9.6 \times 10^{-6} \mu$M $^{-2}$s^{-1}
$[O_2]_k$	O_2 concentration in the astrocyte	200 μM
x_{ki}	Distance between centres of astrocyte and SMC compartments	25 μm
k_{-1}	sGC kinetics rate constant	100 s^{-1}
k_1	sGC kinetics rate constant	2×10^{3} μM $^{-1}$ s^{-1}
k_2	sGC kinetics rate constant	0.1 s^{-1}
k_3	sGC kinetics rate constant	3 μM $^{-1}$ s^{-1}
$V_{\text{max,sGC}}$	Maximal cGMP production rate	0.8520 μM s^{-1}
$K_{\text{m,pde}}$	Michaelis constant	2 μM
k_{dno}	Constant reflecting the activity of various NO scavengers	0.01 s^{-1}
C_4	sGC rate scaling constant	0.011 μM $^{-2}$ s^{-1}
$K_{\text{m,mlcp}}$	Hill coefficient	5.5 μM
k_{pde}	Phosphodiesterase rate constant	0.0195 s^{-1}
x_{ij}	Distance between centres of SMC and EC compartments	3.75 μm
γ_{eNOS}	Relative strength of the Ca^{2+} dependent pathway for eNOS activation	0.1
$\mu_{\text{deact},j}$	eNOS-caveolin association rate	0.0167 s^{-1}
K_{dis}	eNOS-caveolin disassociation rate	0.09 μM s^{-1}

$K_{\text{m,eNOS}}$	Michaelis constant	0.45 μM
$g_{\max}$	Maximum wall-shear-stress-induced eNOS activation	0.06 μM s^{-1}
α_{wss}	Zero shear open channel constant	2
W_0	Shear gating constant	1.4 Pa^{-1}
δ_{wss}	Membrane shear modulus	2.86 Pa
$V_{\text{max,NO},j}$	Maximum catalytic rate of NO production	1.22 s^{-1}
$K_{\text{m,O2},j}$	Michaelis constant for eNOS for O_2	7.7 μM
$[LArg]_j$	L-Arg concentration in the neuron	100 μM
$K_{\text{m,L-Arg},j}$	Michaelis constant for L-Arg	1.5 μM
$\Delta P/L$	Pressure drop over length of arteriole	9.1×10^{-2} Pa μm^{-1}
$k_{\text{O2},j}$	O_2 reaction rate constant	9.6×10^{-6} μM^{-2} s^{-1}
$D_{\text{c,NO}}$	NO diffusion coefficient	3300 $\mu\text{m}^2\text{s}^{-1}$
r_l	Constant of lumen radius	25 μm

Table 11: Parameters of the NO submodel, for references see Dormanns et al. [4].

12 AA 20-HETE NO pathway

In our previous model we noted that the rate of increase of $nNOS_{act}$ and NO was linear and reached a peak at 3 seconds after stimulation. we found a mistake in the NMDA receptor conductance value g_{Ca} (in the code) . This allowed for Ca_{neuron} to be about $6\mu M$ which is similar to that found by [22] for 10 receptors per post-synapse. The new values (in red in Table 11) provide a maximum of $nNOS_{act} = 0.25\mu M$ and a maximum of $NO = 0.13\mu M$.
Our results have so far indicated that the NO-cGMP pathway is very slow (even when using experimental data from [30]). This has led to a reconsideration of the NO model and an investigation into the relationship between NO, as a vasodilator and 20-HETE as a vasoconstrictor. Liu et al [13] pprovides an hypothesis on the relationship between NO and 20-HETE and EETs in neurovascular coupling. This is illustrated in Figure 17. The key for vasoconstriction is the modulation (inhibition) of the K_{Ca} channel by 20-HETE. Whilst in contrast NO in addition to the cGMP pathway inhibits the production of 20-HETE from arachidonic acid (AA) via the CYP4A enzyme. In this hypothesis AA diffuses to the SMC from the astrocyte. Using the model of Haffield et al [7] we can write conservation equations for AA and 20-HETE as shown below.

$$[AA] = [AA]_b + \frac{AA_{max}\Delta[Ca^{2+}]}{AA_M} \tag{208}$$

$$\frac{d}{dt}[20-HETE] = f_{NO}\frac{V_{A11}[AA]}{K_{A11}+[AA]} + \frac{V_{F2}[AA]}{K_{F2}+[AA]} - \mu[20-HETE] \tag{209}$$

$$f_{NO} = \frac{1}{1+exp(\frac{NO_i - NO_{rest}}{R_{NO}})} \tag{210}$$

The first RHS two terms are based on the fact that both CYPA2 and CYPF2 enzymes contribute to the 20-HETE production. Nitric Oxide degrades the CYPA2 enzyme and hence the function f_{NO} provides a phenomenological way of expressing this degradation. The parameter values are given in the Table below

Parameter	Description	Value
$[AA]_b$	archidonic acid baseline	9.3 μm
AA_M	Michaelis constant	0.161 μM
AA_{max}	AA max reaction rate	29 μM

V_{A11}	CYPA 20-HETE max reaction rate	0.212 s^{-1}
K_{A11}	CYPA Michaelis constant	228 μM
V_{F2}	CYPF 20-HETE max reaction rate	0.0319 s^{-1}
K_{F2}	CYPF Michaelis constant	23.5 μM
μ	20-HETE decay constant	0.139 s^{-1}
D_{AA}	Diffusion coefficient of AA [1]	$10^{-8} m^2 s^{-1}$
NO_{rest}	NO resting concentration for f_{NO}	0.02047 μM
R_{NO}	scaling parameter for f_{NO}	0.02 s^{-1}

Table 12: parameter values for the production of archidonic acid and 20-HETE.

13 Wall mechanics

13.1 ODEs

Fraction of free phosphorylated cross-bridges (-):

$$\frac{d[Mp]}{dt} = \chi_w \left(K_4[AMp] + K_1[M] - (K_2 + K_3)[Mp]\right) \tag{211}$$

Fraction of attached phosphorylated cross-bridges (-):

$$\frac{d[AMp]}{dt} = \chi_w \left(K_3[Mp] + K_6[AM] - (K_4 + K_5)[AMp]\right) \tag{212}$$

Fraction of attached dephosphorylated cross-bridges (-):

$$\frac{d[AM]}{dt} = \chi_w \left(K_5[AMp] - (K_7 + K_6)[AM]\right) \tag{213}$$

Vessel radius (μm):

$$\frac{dR}{dt} = \frac{R_{init}}{\eta}\left(\frac{RP_T}{h} - E\frac{R - R_0}{R_0}\right) \tag{214}$$

13.2 Algebraic Variables

Fraction of free non-phosphorylated cross-bridges (-):

$$[M] = 1 - [AM] - [AMp] - [Mp] \tag{215}$$

Rate constants for phosphorylation of M to Mp and of AM to AMp (s^{-1}):

$$K_1 = K_6 = \gamma_{cross} Ca_i^{n_{cross}} \tag{216}$$

Rate constants for dephosphorylation of Mp to M and of AMp to AM (s^{-1}):

$$K_2 = K_5 = \delta_K \left(k_{\text{mlpc,b}} + k_{\text{mlpc,c}} R_{\text{cGMP}}\right) \tag{217}$$

Wall thickness of the vessel (μm):

$$h = 0.1R \tag{218}$$

Fraction of attached myosin cross-bridges (-):

$$F_r = [AM_p] + [AM] \tag{219}$$

[1] Kong et al Fluid Phase Equilibria, **297**(3)pp 162-167

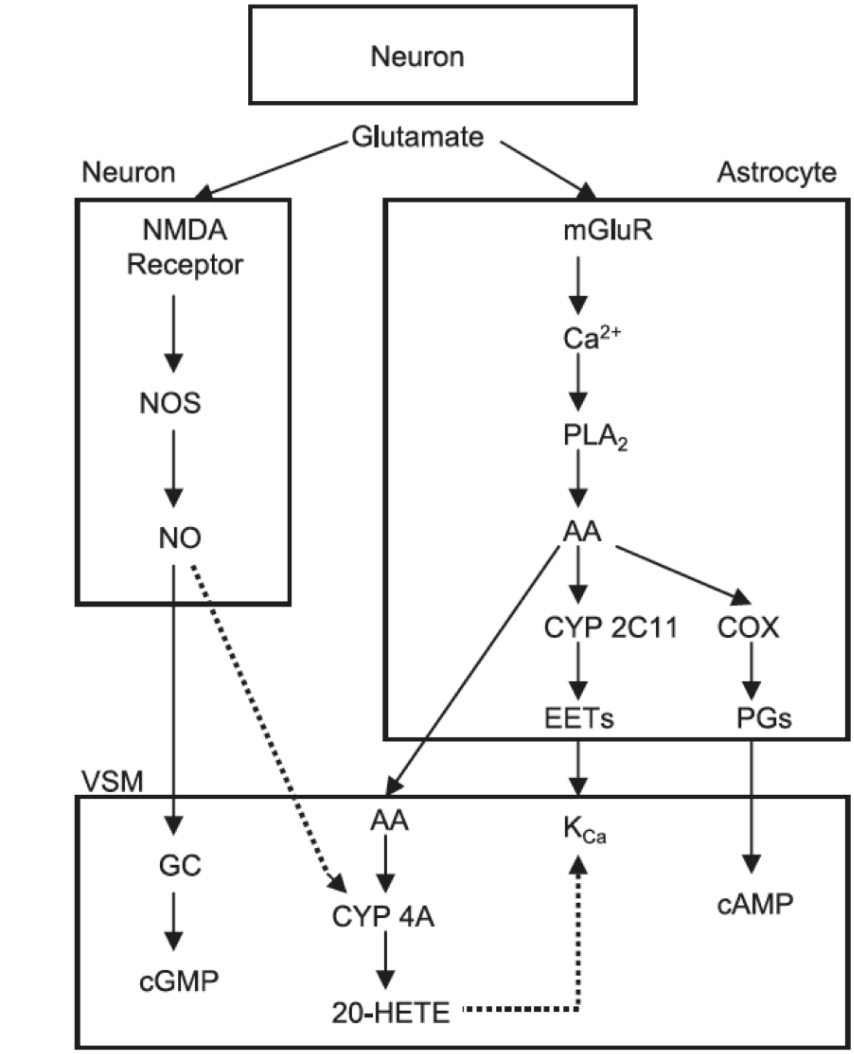

Figure 17: proposed pathway sketch by Liu et al [13] of 20-HETE and NO. Dashed lines are inhibition

Young's modulus (Pa):

$$E = E_{pas} + F_r \left(E_{act} - E_{pas}\right) \tag{220}$$

Initial radius (μm):

$$R_0 = R_{init} + F_r(\alpha_R - 1)R_{init} \tag{221}$$

Parameter	Description	Value
χ_w	Scaling constant for wall mechanics	1.7
K_3	Rate constant for attachment of phosphorylated crossbridges	0.4 s^{-1}
K_4	Rate constant for detachment of phosphorylated crossbridges	0.1 s^{-1}
K_7	Rate constant for detachment of dephosphorylated crossbridges	0.1 s^{-1}
γ_{cross}	Sensitivity of the contractile apparatus to Ca^{2+}	17 $\mu M^{-3} s^{-1}$
n_{cross}	Fraction constant of the phosphorylation crossbridge	3
δ_K	Constant to fit data	58.14
$k_{\text{mlpc,b}}$	Basal MLC dephosphorylation rate constant	8.6×10^{-3} s^{-1}
$k_{\text{mlpc,c}}$	First-order rate constant for cGMP regulated MLC dephosphorylation	32.7×10^{-3} s^{-1}

η	Viscosity	10^4 Pa s
P_T	Transmural pressure	4×10^3 Pa
E_{pas}	Young's moduli for the passive vessel	66×10^3 Pa
E_{act}	Young's moduli for the active vessel	233×10^3 Pa
α_R	Scaling factor for initial radius	0.6

Table 13: Parameters of the wall mechanics submodel, for references see Dormanns et al. [5].

14 BOLD response

14.1 ODEs

The non dimensional cerebral blood volume (CBV) (-):

$$\frac{d\text{CBV}}{dt} = \frac{1}{\tau_{MTT} + \tau_{TAT}} \left(f_{in} - \text{CBV}^{\frac{1}{d}} \right) \tag{222}$$

with $f_{in} = \frac{CBF}{CBF_{init}}$

The non dimensional deoxyhemoglobin (HbR) concentration (-):

$$\frac{d\text{HbR}}{dt} = \frac{1}{\tau_{MTT}} \left(\frac{f_{in} E(t)}{E_0} - \frac{\text{HbR}}{\text{CBV}} f_{out} \right) \tag{223}$$

$$f_{out} = CBV^{\frac{1}{d}} + \tau_{TAT} \frac{dCBV}{dt} \tag{224}$$

Here f_{out} is the flow out of the veinous balloon.

14.2 Algebraic Variables

The non dimensional normalised total hemoglobin (HbT) concentration (-):

$$\text{HbR}_N = \frac{\text{HbR}_N}{\text{HbR}(0)} \tag{225}$$

$$\text{HbT}_N = \frac{\text{CBF}_N \text{HbR}_N}{\text{CMRO}_{2_N}} \tag{226}$$

where the normalised CBF is given by $\text{CBF}_N = \text{CBF/CBF}(0)$ and $\text{CBF}(0)$ is the steady state value, similarly for HbR. $CMRO2 = f_{in} \frac{E(t)}{E_0}$ and $CMRO2_0 = 1$, hence

$$\begin{aligned} HbT_N &= CBF_N HbR_N \frac{E_0}{f_{in} E(t)} \\ &= HbR \frac{E_0}{E(t)} \end{aligned} \tag{227}$$

.

The non dimensional normalised oxyhemoglobin (HbO) concentration (-):

$$\text{HbO}_N = \text{HbT}_N - \text{HbR}_N + 1 \tag{228}$$

The BOLD signal change from its steady state value (-):

$$\Delta BOLD \approx V_0 \left(a_1 \left[1 - \text{HbR}_N \right] + a_2 \left[\text{CBV}_N - 1 \right] \right) \tag{229}$$

Parameter	Description	Value
τ_{MTT}	Mean transit time	3 s
τ_{TAT}	Transient adjustment time constant	20 s
d	Empirical relation between CBF and CBV	2.5
a_1	Weight for HbR change	3.4
a_2	Weight for CBV change	1
V_0	Resting venous blood volume fraction	0.03
E_0	Baseline oxygen extraction fraction	0.4

Table 14: Parameters of the BOLD submodel, for references see Mathias et al. [16].

15 Tissue Slice Model

15.1 ODEs

K^+ concentration in the astrocyte of NVU block i with four neighbours j (μM):

$$\frac{dK_k^i}{dt} = -\frac{1}{\Delta x}\sum_j J_{K,i\to j} - J_{K_k}^i + 2J_{NaK_k}^i + J_{NKCC1_k}^i + J_{KCC1_k}^i \tag{230}$$

Membrane potential in the astrocyte of NVU block i with four neighbours j (mV):

$$\frac{dv_k^i}{dt} = \gamma_v \left[-\frac{1}{\Delta x}\sum_j z_K J_{K,i\to j} - J_{BK_k}^i - J_{K_k}^i - J_{Cl_k}^i - J_{NBC_k}^i - J_{Na_k}^i - J_{NaK_k}^i - 2J_{TRPV_k}^i \right] \tag{231}$$

K^+ concentration in the ECS of NVU block i with four neighbours j (mM):

$$\frac{dK_e^i}{dt} = -\frac{1}{\Delta x}\sum_j J_{K,i\to j}^e + \frac{1}{Ff_e}\left(\frac{A_s I_{K,tot_{sa}}^i}{V_s} + \frac{A_d I_{K,tot_d}^i}{V_d}\right) - \frac{d\text{Buff}_e^i}{dt} \tag{232}$$

Na^+ concentration in the ECS of NVU block i with four neighbours j (mM):

$$\frac{dNa_e^i}{dt} = -\frac{1}{\Delta x}\sum_j J_{Na,i\to j}^e + \frac{1}{Ff_e}\left(\frac{A_s I_{Na,tot_{sa}}^i}{V_s} + \frac{A_d I_{Na,tot_d}^i}{V_d}\right) \tag{233}$$

15.2 Algebraic Variables

Gap junction flux of K_k from NVU block i to neighbour j (μMm s^{-1}):

$$J_{K,i\to j} = -\frac{D_{gap}}{\Delta x^2}\left((K_k^j - K_K^i) + \frac{z_K F}{RT}\frac{K_k^i + K_k^j}{2}(v_k^j - v_k^i)\right) \tag{234}$$

Extracellular electrodiffusive flux of K_e and Na_e from NVU block i to neighbour j (mMm s^{-1}):

$$J_{K,i\to j}^e = -\frac{D_{K,e}}{\Delta x}\left[(K_e^j - K_e^i) - z_K\left(\frac{K_e^i + K_e^j}{2}\right)\left(\frac{z_K D_{K,e}(K_e^j - K_e^i) + z_{Na} D_{Na,e}(Na_e^j - Na_e^i)}{z_K^2 D_{K,e}\frac{K_e^i + K_e^j}{2} + z_{Na}^2 D_{Na,e}\frac{Na_e^i + Na_e^j}{2}}\right)\right] \tag{235}$$

$$J_{Na,i\to j}^e = -\frac{D_{Na,e}}{\Delta x}\left[(Na_e^j - Na_e^i) - z_{Na}\left(\frac{Na_e^i + Na_e^j}{2}\right)\left(\frac{z_K D_{K,e}(K_e^j - K_e^i) + z_{Na} D_{Na,e}(Na_e^j - Na_e^i)}{z_K^2 D_{K,e}\frac{K_e^i + K_e^j}{2} + z_{Na}^2 D_{Na,e}\frac{Na_e^i + Na_e^j}{2}}\right)\right] \tag{236}$$

Parameter	Description	Value
D_{gap}	Astrocytic gap junction diffusion coefficient	3.1×10^{-9} m^2 s^{-1}
Δx^2	Width of one NVU block	1.24×10^{-4} m
$D_{K,e}$	Extracellular K^+ diffusion coefficient	3.8×10^{-9} m^2 s^{-1}
$D_{Na,e}$	Extracellular Na^+ diffusion coefficient	2.5×10^{-9} m^2 s^{-1}

Table 15: Parameters of the large scale tissue slice model.

16 Initial values (before we optimise ?)

These initial values take into account the new $nNOS_{act_j}$ and NO equations. All concentrations are in micromolar and membrane potential in millivolts.

16.1 Neuron

E_t = 0; I_t = 0; K_e = 3.5; Na_{sa} = 9.37; Na_d = 9.42; $O2$ = 0.02566; CBV = 1.204; HbR = 0.7641; Ca_n = 0.1; $nNOS_{act_n}$ = 0.01056; NO_n = 0.02425;

16.2 Astrocyte

Na_k = 18740; K_k = 92660; HCO_{3_k} = 9085; Cl_k = 8212; Na_s = 149200; K_s = 2932; HCO_{3_s} = 16980; K_p = 3039; w_k = 8.26e-5; Ca_k = 0.1435; s_k = 480.8; h_k = 0.4107; I_k = 0.048299; eet_k = 0.4350; m_k = 0.513; Ca_p = 1853; NO_k = 0.02234; v_k = -88.79;

16.3 SMC/EC

Ca_i = 0.2641; s_i = 1.1686; v_i = -34.7; w_i = 0.2206; I_i = 0.275; K_i = 99994.8; NO_i = 0.02047; E_b = 0.6372; E_6c = 0.2606; $cGMP_i$ = 6.1; Ca_j = 0.8339; s_j = 0.6262; v_j = -68.39; I_j = 0.825; $eNOS_{act_j}$ = 0.4451; NO_j = 0.02051;

References

[1] Adamchik, D. A., Matrosov, V. V., and Kazantsev, V. B. (2018). Emergence of Relaxation Oscillations in Neurons Interacting With Non-stationary Ambient GABA. *Frontiers in Computational Neuroscience*, 12(April):1–10.

[2] Anenberg, E., Chan, A. W., Xie, Y., LeDue, J. M., and Murphy, T. H. (2015). Optogenetic stimulation of GABA neurons can decrease local neuronal activity while increasing cortical blood flow. *Journal of Cerebral Blood Flow and Metabolism*, 35(10):1579–1586.

[3] Biscoe, T. and Duchan, M. (1985). The anion selectivity of gaba-mediated post synaptic potentials in mouse hippocampus cells. *Quarterly Journal of Experimental Physiology*, 70:305.

[4] Dormanns, K., Brown, R. G., and David, T. (2016). The role of nitric oxide in neurovascular coupling. *Journal of theoretical biology*, 394:1–17.

[5] Dormanns, K., van Disseldorp, E. M. J., Brown, R. G., and David, T. (2015). Neurovascular coupling and the influence of luminal agonists via the endothelium. *Journal of Theoretical Biology*, 364:49–70.

[6] Farr, H. and David, T. (2011). Models of neurovascular coupling via potassium and EET signalling. *Journal of theoretical biology*, 286(1):13–23.

[7] Hadfield, J., Plank, M. J., and David, T. (2013). Modeling Secondary Messenger Pathways in Neurovascular Coupling. *Bulletin of Mathematical Biology*, 75(3):428–443.

[8] Jayakumar, A. R., Sujatha, R., Paul, V., Asokan, C., Govindasamy, S., and Jayakumar, R. (1999). Role of nitric oxide on GABA, glutamic acid, activities of GABA-T and GAD in rat brain cerebral cortex. *Brain Research*, 837(1-2):229–235.

[9] Kelsom, C. and Lu, W. (2013). Development and specification of GABAergic cortical interneurons. *Cell and Bioscience*, 3(1):1.

[10] Kenny, A., Plank, M. J., and David, T. (2018). The role of astrocytic calcium and TRPV4 channels in neurovascular coupling. *Journal of Computational Neuroscience*, 44(1):97–114.

[11] Koenigsberger, M., Sauser, R., Bény, J.-L. J. L., and Meister, J.-J. J. J.-J. (2006). Effects of arterial wall stress on vasomotion. *Biophysical journal*, 91(September):1663–1674.

[12] Koenigsberger, M., Sauser, R., Lamboley, M., Bény, J.-L. L., Meister, J.-J. J., and Be, J.-l. (2004). Ca2+ dynamics in a population of smooth muscle cells: modeling the recruitment and synchronization. *Biophysical Journal*, 87(1):92–104.

[13] Liu, X., Li, C., Falck, J. R., Roman, R. J., Harder, D. R., and Koehler, R. C. (2008). Interaction of nitric oxide, 20-HETE, and EETs during functional hyperemia in whisker barrel cortex. *American journal of physiology. Heart and circulatory physiology*, 295(2):H619—-31.

[14] Losi, G., Mariotti, L., and Carmignoto, G. (2014). GABAergic interneuron to astrocyte signalling: A neglected form of cell communication in the brain. *Philosophical Transactions of the Royal Society B: Biological Sciences*, 369(1654).

[15] Mathias, E., Kenny, A., Plank, M. J., and David, T. (2018). Integrated models of neurovascular coupling and BOLD signals: Responses for varying neural activations. *NeuroImage*, 174(March):69–86.

[16] Mathias, E. J., Plank, M. J., and David, T. (2017). A model of neurovascular coupling and the BOLD response: PART I. *Computer Methods in Biomechanics and Biomedical Engineering*, 20(5):508–518.

[17] Mizuta, K., Xu, D., Pan, Y., Comas, G., Sonett, J. R., Zhang, Y., Panettieri, R. A., Yang, J., and Emala, C. W. (2008). GABA A receptors are expressed and facilitate relaxation in airway smooth muscle . *American Journal of Physiology-Lung Cellular and Molecular Physiology*, 294(6):L1206–L1216.

[18] Ostby, I., Oyehaug, L., Einevoll, G. T., Nagelhus, E. A., Plahte, E., Zeuthen, T., Lloyd, C. M., Ottersen, O. P., and Ombolt, S. W. (2009). Astrocytic Mechanisms Explaining Neural-Activity- Induced Shrinkage of Extraneuronal Space. *PLoS Comput. Biol*, 5(1):1–12.

[19] Paul, V. and Jayakumar, A. R. (2000). A role of nitric oxide as an inhibitor of γ-aminobutyric acid transaminase in rat brain. *Brain Research Bulletin*, 51(1):43–46.

[20] Petroff, O. A. (2002). GABA and glutamate in the human brain. *Neuroscientist*, 8(6):562–573.

[21] Samardzic, J., Dragana, J., Hencic, B., Jasna, J., and Svob Strac, D. (2016). GABA/Glutamate Balance: A Key for Normal Brain Functioning. In *Intech*, volume i, page 13.

[22] Santucci, D. M. and Raghavachari, S. (2008). The effects of NR2 subunit-dependent NMDA receptor kinetics on synaptic transmission and CaMKII activation. *PLoS Computational Biology*, 4(10).

[23] Schmidt-Wilcke, T., Fuchs, E., Funke, K., Vlachos, A., Muller-Dahlhaus, F., Puts, N. A. J., Harris, R. E., and Edden, R. A. E. (2018). GABA — from Inhibition to Cognition: Emerging Concepts. *The Neuroscientist*, 24(5):501–515.

[24] Schousboe, A., Bak, L., and Waagepetersen, H. (2013). Astrocytic control of biosynthesis and turnover of the neurotransmitters glutamate and gaba. *Frontiers in Endocrinology*, 4:102.

[25] Sherif, F. M. and Saleem Ahmed, S. (1995). Basic aspects of GABA-transaminase in neuropsychiatric disorders. *Clinical Biochemistry*, 28(2):145–154.

[26] Shyamaladevi, N., Jayakumar, A. R., Sujatha, R., Paul, V., and Subramanian, E. H. (2002). Evidence that nitric oxide production increases γ-amino butyric acid permeability of blood-brain barrier. *Brain Research Bulletin*, 57(2):231–236.

[27] Uhlirova, H., Kivilvim, K., Tian, P., Thunemann, M., Desjardins, M., Saisan, P. A., Sakadzic, S., Ness, T. V., Mateo, C., Cheng, Q., Weldy, K. L., Razoux, F., Vandenberghe, M., Cremonesi, J. A., Ferri, C. G. L., Nizar, K., Sridhar, V. B., Steed, T. C., Abashin, M., Fainman, Y., Masliah, E., Djurovic, S., Andreassen, O. A., Silva, G. A., Boas, D. A., Kleinfeld, D., Buxton, R. B., Einevol, G. T., Dale, A. M., and Devor, A. (2016). Cell type specificity of neurovascular coupling in cerebral cortex. *eLife (supplemetary material)*, 5(MAY2016):1–23.

[28] Vega Rasgado, L. A., Reyes, G. C., and Vega Díaz, F. (2018). Role of nitric oxide synthase on brain GABA transaminase activity and GABA levels. *Acta Pharmaceutica*, 68(3):349–359.

[29] Xiong, Z., Bolzon, B. J., and Cheung, D. W. (1993). Neuropeptide Y potentiates calcium-channel currents in single vascular smooth muscle cells. *Pflugers Archiv European Journal of Physiology*, 423:504–510.

[30] Yang, J., Clark, J. W., Bryan, R. M., and Robertson, C. (2003). The myogenic response in isolated rat cerebrovascular arteries: smooth muscle cell model. *Medical Engineering & Physics*, 25(8):691–709.

[31] You, J., Edvinsson, L., and Bryan, R. M. (2001). Neuropeptide Y-mediated constriction and dilation in rat middle cerebral arteries. *Journal of Cerebral Blood Flow and Metabolism*, 21(1):77–84.

[32] Zheng, Y., Pan, Y., Harris, S., Billings, S., Coca, D., Berwick, J., Jones, M., Kennerley, A., Johnston, D., Martin, C., Devonshire, I. M., and Mayhew, J. (2010). A dynamic model of neurovascular coupling: Implications for blood vessel dilation and constriction. *NeuroImage*, 52(3):1135–1147.